consistent with the hypothesis that *Sukumo* extract interferes with virions rather than cell function. It might also explain why *Sukumo* extract is less toxic to target cells in vitro.

The biochemical features of water extract of *Sukumo* prepared from *Polygonum tinctorium* that selectively inhibited the replication of HIV-1 were studied. The anti-viral activity was extracted from *Sukumo* in a variety of ways, using water and organic solvents (hexane, chloroform, acetone and ethanol). Inhibitory activity was found in the aqueous extracts, whereas the extracts by organic solvents did not show any anti-HIV activity. Indigo, a staining ingredient and tryptanthrin, a low molecular weight component from *Polygonum tinctorium*, also did not exihibit any anti-HIV activity (data not shown).

The main fraction of anti-HIV activity was eluted from the DEAE-Sephacel column, a negative ion-exchange column at higher molar (1.0–2.0) NaCl. This result indicate that the active factor(s) is highly anionic. It was also confirmed that the anti-HIV compound(s) consist of phenolic substructure by $FeCl_3$–$K_3Fe(CN)_6$ staining (Barton et al., 1952) (data not shown) and a polysaccharide containing sulfur atom by sugar analysis and elemental analysis, respectively (Table 1). The factor was estimated to be a high molecular weight compound of 10,000–50,000 by Sephadex G-75 gel-filtration analysis (data not shown) and an SDS-gel of *Sukumo* extract (Fig. 6B). No protein was detected in the water extract of *Sukumo* with SDS-PAGE/silver staining. The data confirm our observation that the inhibitory activity of *Sukumo* extract was not inactivated by protease digestion or heating at 121 °C for 20 min. Furthermore, boiling of the *Sukumo* extract in the presence of 1N HCl, 6N H_2SO_4 and 1N NaOH for 6 h did not result in any loss of this activity. Similarly, it was not inactivated by $NaIO_4$ treatment (Nakashima et al., 1987b), which breaks down carbohydrates (Table 2). This suggests that the sugar backbone is not essential for the anti-HIV activity of the *Sukumo* extract. The pharmaceutical value of the *Sukumo* extract is likely to be further enhanced by its stability over a wide range of pH values, as shown by the heating at 121 °C 20 min and treatment with acid and alkaline conditions. Since the anti-HIV-1 activity of *Sukumo* was higher than that of fresh leaves (data not shown), the possibility that the active substances were derived from bacteria could not be excluded.

We compared difference between representative sulfated polysaccharides and *Sukumo* extract for their susceptibility to acid treatment. The anti-HIV-1 effect was clearly abrogated by this treatment in the case of dextran sulfate and heparin, but not *Sukumo* extract (Table 2). The anti-HIV-1 activity of heparin was completely destroyed by 6N H_2SO_4 treatment as in the case of 1N HCl treatment of dextran sulfate. Unlike epigallocatechin gallate, a polyphenolic substance from green tea (Suzutani et al., 2003; Yamaguchi et al., 2002), *Sukumo* extract did not exert any anti-HIV-1 activity on the post-virus entry process. Further work on the characterization of the *Sukumo* extract and its potency as an anti-viral candidate drug is in progress.

Acknowledgements

The authors thank Dr. Fumio Shaku for performing the infection of HSV-1 experiments and gift of wild-type herpes simplex virus 1 and Vero cells. This work was supported by grants from the Ministry of Education, Science, and Culture and the Ministry of Health, Labor, and Welfare of Japan. The manuscript was reviewed prior to submission by Pacific Edit.

References

Baba, M., Pauwels, R., Balzarini, J., Arnout, J., Desmyter, J., De Clercq, E., 1988. Mechanism of inhibitory effect of dextran sulfate and heparin on replication of human immunodeficiency virus in vitro. Proc. Natl. Acad. Sci. U.S.A. 85, 6132–6136.

Bartolini, B., Di Caro, A., Cavallaro, R.A., Liverani, L., Mascellani, G., La Rosa, G., Marianelli, C., Muscillo, M., Benedetto, A., Cellai, L., 2003. Susceptibility to highly sulphated glycosaminoglycans of human immunodeficiency virus type 1 replication in peripheral blood lymphocytes and monocyte-derived macrophages cell cultures. Antiviral Res. 58, 139–147.

Barton, G.M., Evans, R.S., Gardner, J.A.F., 1952. Paper chromatography of phenolic substances. Nature 170, 249–250.

Honda, G., Tabata, M., 1979. Isolation of antifungal principle tryptathrin, from *Strobilanthes cusia O. Kuntze*. Planta Med. 36, 85–86.

Ichiyama, K., Yokoyama-Kumakura, S., Tanaka, Y., Tanaka, R., Hirose, K., Bannai, K., Edamatsu, T., Yanaka, M., Niitani, Y., Miyano-Kurosaki, N., Takaku, H., Koyanagi, Y., Yamamoto, N., 2003. A duodenally absorbable CXC chemokine receptor 4 antagonist, KRH-1636, exhibits a potent and selective anti-HIV-1 activity. Proc. Natl. Acad. Sci. U.S.A. 100, 4185–4190.

Kataoka, M., Hirata, K., Kunikata, T., Ushio, S., Iwaki, K., Ohashi, K., Ikeda, M., Kurimoto, M., 2001. Antibacterial action of tryptanthrin and kaempferol, isolated from the indigo plant (*Polygonum tinctorium* Lour.), against Helicobacter pylori-infected Mongolian gerbils. J. Gastroenterol. 36, 5–9.

Kim, H.M., Hong, D.R., Lee, E.H., 1998. Inhibition of mast cell-dependent anaphylactic reactions by the pigment of *Polygonum tinctorium* (Chung-Dae) in rats. Gen. Pharmacol. 31, 361–365.

Koya-Miyata, S., Kimoto, T., Micallef, M.J., Hino, K., Taniguchi, M., Ushio, S., Iwaki, K., Ikeda, M., Kurimoto, M., 2001. Prevention of azoxymethane-induced intestinal tumors by a crude ethyl acetate-extract and tryptanthrin extracted from *Polygonum tinctorium* Lour. Anticancer Res. 21, 3295–3300.

Lin, Y.L., Mettling, C., Portales, P., Reynes, J., Clot, J., Corbeau, P., 2002. Cell surface CCR5 density determines the postentry efficiency of R5 HIV-1 infection. Proc. Natl. Acad. Sci. U.S.A. 99, 15590–15595.

Miyake, M., Arai, N., Ushio, S., Iwaki, K., Ikeda, M., Kurimoto, M., 2003. Promoting effect of kaempferol on the differentiation and mineralization of murine pre-osteoblastic cell line MC3T3-E1. Biosci. Biotechnol. Biochem. 67, 1199–1205.

Moore, J.P., Stevenson, M., 2000. New targets for inhibitors of HIV-1 replication. Nat. Rev. Mol. Cell Biol. 1, 40–49.

Moulard, M., Lortat-Jacob, H., Mondor, I., Roca, G., Wyatt, R., Sodroski, J., Zhao, L., Olson, W., Kwong, P.D., Sattentau, Q.J., 2000. Selective interactions of polyanions with basic surfaces on human immunodeficiency virus type 1 gp120. J. Virol. 74, 1948–1960.

Nakashima, H., Kido, Y., Kobayashi, N., Motoki, Y., Neushul, M., Yamamoto, N., 1987a. Purification and characterization of an avian myeloblastosis and human immunodeficiency virus reverse transcriptase inhibitor, sulfated polysaccharides extracted from sea algae. Antimicrob. Agents Chemother. 31, 1524–1528.

Nakashima, H., Kido, Y., Kobayashi, N., Motoki, Y., Neushul, M., Yamamoto, N., 1987b. Antiretroviral activity in a marine red alga: reverse transcriptase inhibition by an aqueous extract of *Schizymenia pacifica*. J. Cancer Res. Clin. Oncol. 113, 413–416.

Nakashima, H., Yoshida, O., Baba, M., De Clercq, E., Yamamoto, N., 1989. Anti-HIV activity of dextran sulphate as determined under different experimental conditions. Antiviral Res. 11, 233–246.

Nakashima, H., Murakami, T., Yamamoto, N., Sakagami, H., Tanuma, S., Hatano, T., Yoshida, T., Okuda, T., 1992. Inhibition of human immunodeficiency viral replication by tannins and related compounds. Antiviral Res. 18, 91–103.

Santhosh, K.C., Paul, G.C., De Clercq, E., Pannecouque, C., Witvrouw, M., Loftus, T.L., Turpin, J.A., Buckheit Jr., R.W., Cushman, M., 2001. Correlation of anti-HIV activity with anion spacing in a series of cosalane analogues with extended polycarboxylate pharmacophores. J. Med. Chem. 44, 703–714.

Suzutani, T., Ogasawara, M., Yoshida, I., Azuma, M., Knox, Y.M., 2003. Anti-herpesvirus activity of an extract of *Ribes nigrum* L. Phytother. Res. 17, 609–613.

Witvrouw, M., De Clercq, E., 1997. Sulfated polysaccharides extracted from sea algae as potential antiviral drugs. Gen. Pharmacol. 29, 497–511.

Yamaguchi, K., Honda, M., Ikigai, H., Hara, Y., Shimamura, T., 2002. Inhibitory effects of (−)-epigallocatechin gallate on the life cycle of human immunodeficiency virus type 1 (HIV-1). Antiviral Res. 53, 19–34.

Ylisastigui, L., Bakri, Y., Amzazi, S., Gluckman, J.C., Benjouad, A., 2000. Soluble glycosaminoglycans do not potentiate RANTES antiviral activity on the infection of primary macrophages by human immunodeficiency virus type 1. Virology 278, 412–422.

Zacharius, R.M., Zell, T.E., Morrison, J.H., Woodlock, J.J., 1969. Glycoprotein staining following electrophoresis on acrylamide gels. Anal Biochem. 30, 148–152.

Antiviral Chemistry & Chemotherapy 16:363–373

A novel small molecular weight compound with a carbazole structure that demonstrates potent human immunodeficiency virus type-1 integrase inhibitory activity

Hua Yan[1], Tomoko Chiba Mizutani[1], Nobuhiko Nomura[2], Tadakazu Takakura[2], Yoshihiro Kitamura[3], Hideka Miura[1], Masako Nishizawa[1], Masashi Tatsumi[1], Naoki Yamamoto[1] and Wataru Sugiura[1*]

[1]AIDS Research Center, National Institute of Infectious Diseases, Tokyo, Japan
[2]Research and Discovery Laboratories, Toyama Chemical Co. Ltd., Toyama, Japan
[3]Division of Infectious Diseases, Advanced Clinical Research Center, Institute of Medical Science, University of Tokyo, Japan.

*Corresponding author: Tel: +81 42 561 0771; Fax: +81 42 561 7746; E-mail: wsugiura@nih.go.jp

The integration of reverse transcribed proviral DNA *into a host genome* is an essential event in the human immunodeficiency virus type 1 (HIV-1) replication life cycle. Therefore, the viral enzyme integrase (IN), which plays a crucial role in the integration event, has been an attractive target of anti-retroviral drugs. Several IN inhibitory compounds have been reported previously, yet none has been successful in clinical use. To find a new, more successful IN inhibitor, we screened a diverse library of 12 000 small molecular weight compounds randomly by *in vitro* strand-transfer assay. We identified a series of substituted carbazoles that exhibit strand-transfer inhibitory activity at low micromolar concentrations. Of these, the most potent compound exhibited an IC_{50} of 5.00 ±3.31 μM (CA-0). To analyse the structural determinants of strand-transfer inhibitory activity of the carbazole derivatives, we selected 23 such derivatives from our compound library and performed further analyses. Of these 23 compounds, six showed strong strand-transfer inhibition. The inhibition kinetics analyses and ethidium bromide displacement assays indicated that the carbazole derivatives are competitive inhibitors and not intercalators. An HeLa4.5/LTR-nEGFP cell line was employed to evaluate *in vitro* virus replication inhibition of the carbazole derivatives, and IC_{50} levels ranged from 0.48–1.52 μM. Thus, it is possible that carbazole derivatives, which possess structures different from previously-reported IN inhibitors, may become novel lead compounds in the development of IN inhibitors.

Keywords: integrase inhibitor, carbazole, HIV-1, antiretroviral drug

Introduction

Human immunodeficiency virus type 1 (HIV-1), causative agent of acquired immunodeficiency syndrome (AIDS), possesses three critical enzymes for replication. These are protease (PR), reverse transcriptase (RT), and integrase (IN) (Ruscetti, 1985; Kohl *et al.*, 1988; LaFemina *et al.*, 1992). As inactivating any of these enzymes may negate the infectivity of HIV-1, the enzymes have been targets of anti-retroviral drug development. Indeed, great progress in anti-retroviral drug discovery has been achieved in recent decades, and today 10 RT inhibitors and eight PR inhibitors (De Clercq, 1992; Tronchet & Seman, 2003; Balzarini, 2004; Imamichi, 2004) are available for anti-retroviral treatments. The third enzyme, IN, has also been a major target of inhibitor development. L-708,906 and L-731,988, which possess diketo acid moieties within their structures, were the first IN-specific inhibitors discovered (Pommier *et al.*, 2000; Dayam & Neamati, 2003; Pluymers *et al.*, 2002; Hazuda *et al.*, 2000). S-1360 and L-870,810, which also have diketo acid moieties, are IN inhibitors that have reached clinical Phase I/II trials for the first time (Johnson *et al.*, 2004; Hazuda *et al.*, 2004). However, although there have been large advances in the development of IN inhibitors, further research and analysis is required to develop clinically usable compounds.

Integrase (IN), the leading target of novel anti-retroviral inhibitor development, is the enzyme responsible for integration, wherein reverse transcribed HIV-DNA is inserted into a host genome, and is critical for viral replication, which in turn establishes latency and chronic infection (Chun *et al.*, 1995). IN is composed of three distinct

domains – the N-terminal domain (amino acids 1–50) with a zinc-binding motif (Schauer & Billich, 1992; Burke *et al.*, 1992), the catalytic core domain (amino acids 50–212) with polynucleotidyl transfer activity and sequence-specific endonuclease activity (Engelman & Craigie, 1992; Engelman *et al.*, 1994) and the C-terminal domain (amino acids 212–288), which has been thought to relate to nonspecific DNA binding (Khan *et al.*, 1991; Woerner & Marcus-Sekura, 1993).

At present, the function and structure of each domain has not been fully understood. The most well-analysed domain is the catalytic core domain, and its active site has highly conserved amino acidic residues Asp64, Asp116 and Glu152, which are critical for polynucleotidyl transfer activity (LaFemina *et al.*, 1992; Engelman *et al.*, 1995). Previously reported potent IN inhibitors L-708,906, L-731,988, L-801,810, S-1360 and 5-CITEP are all targeted to this domain. These inhibitors bind to the active site, displace divalent metal ion Mg^{2+} from the active site and inactivate the catalytic activity of IN (Grobler *et al.*, 2002; Dayam & Neamati, 2003; Goldgur *et al.*, 1999; Johnson *et al.*, 2004). No specific inhibitors have been reported for the N-terminal and C-terminal domains.

In the present study we attempted to identify novel IN inhibitory compounds, and therefore we conducted a random screening of a library of small molecular weight compounds. As a result, we discovered a series of novel IN inhibitory compounds with carbazole structures, that are quite different from previously reported inhibitory compounds.

Materials and methods

Preparation of integrase

The sequence coding the NL4-3 integrase (IN) was cloned into pET28b(+) (Novagen, Madison, WI, USA), generating pET-IN that codes NL4-3 IN with a hexa-histidine tag at the N-terminus. *Escherichia coli* strain Rosetta (DE3) (Novagen) transformed with pET-IN was grown in 1 l of Super Broth (Biofluids, Camarillo, CA, USA) containing 100 μg/ml kanamycin at 30°C until the optical density of the culture had reached between 0.5 and 0.7 at 600 nm. The recombinant protein expression was induced by isopropyl-1-thio-D-galactopyranoside. After incubation for 3 h, the cells were harvested and resuspended in 100 ml of preparation buffer (20 mM Tris-HCl, pH 8.0, 0.5 M NaCl) and disrupted by sonication. Following high-speed centrifugation at 40 000×g for 45 min at 4°C, the pellet was homogenized in GBB buffer (50 mM Tris-HCl, pH 8.0, 6 M Guanidine HCl and 2 mM 2-ME). The residual pellet was again sonicated and centrifuged at 40 000×g for 30 min at 4°C.

The supernatant was filtered through a 0.22 μm filter and mixed with 1 ml of nickel-affinity resin (Sigma, St. Louis, MO, USA), and incubated overnight at 4°C. The resin was washed twice by mixing with 20 ml of GBB containing 5 mM imidazole (Sigma). The protein was eluted with GBB containing 1 M imidazole. The fractions containing integrase were pooled and 0.5 M EDTA was added to a final concentration of 5 mM. This eluted protein was then sequentially dialysed against (i) 6 M guanidine HCl, 50 mM Tris-HCl (pH 8.0), 2 mM 2-ME, 1 mM EDTA for 2 h at room temperature, (ii) 6 M guanidine HCl, 50 mM Tris-HCl (pH 8.0), 10 mM DTT, 1 mM EDTA for 16 h at room temperature, (iii) 4 M urea, 50 mM Tris-HCl (pH 8.0), 0.5 M NaCl, 1 mM DTT, 0.1 mM EDTA for 16 h at 4°C, (iv) 2 M urea, 50 mM Tris-HCl (pH 8.0), 0.5 M NaCl, 1 mM DTT, 0.1 mM EDTA, 20% (w/v) glycerol for 16 h at 4°C, (v) 1 M urea, 50 mM Tris-HCl (pH 8.0), 1 M NaCl, 1 mM DTT, 0.1 mM EDTA, 15 mM 3-[(3-cholamidopropyl) dimethylammonio]-1-propanesulfonate (CHAPS), 20% (w/v) glycerol for 16 h at 4°C, and (vi) 50 mM Tris-HCl (pH 8.0), 1 M NaCl, 1 mM DTT, 0.1 mM EDTA, 15 mM CHAPS, 20% (w/v) glycerol for 16 h at 4°C. The final preparation was stored at –80°C.

The purified enzyme activity was confirmed and evaluated by strand-transfer assay using M8 apparatus (IGEN, Gaithersburg, MD, USA).

Preparation of test compounds

A diverse library of 12 000 small-molecule compounds was supplied by Toyama Chemicals Co. Ltd. (Toyama, Japan). All test compounds were dissolved in DMSO and adjusted to 2 mM concentration. S-1360 was synthesized as positive control for strand transfer assay.

Construction of strand-transfer assay

Two different strand-transfer assay systems were employed in the IN inhibitor screening trial. For the first screening step, an M8 apparatus and strand-transfer assay kit, ORIGEN HIV integrase assay (IGEN), was used. In brief, magnetic beads coated with 29 mer donor double-stranded DNA (dsDNA) were mixed with purified IN (15 pmol), followed by adding the test compound and 20 mer target dsDNA tagged with ruthenium, conducting electronically inducible fluorescence chemistry, and incubating for 1 h at 37°C. Subsequently, the entire reaction solution was applied to the M8 apparatus, and then strand-transfer products were captured by a magnet in the flow-circuit of the equipment. The amount of the strand-transfer product was measured by ruthenium fluorescence activity. For the second and later screening steps, in-house strand-transfer assay was employed. The in-house assay was designed in 96-well plate format to achieve high-throughput screening.

The following donor and target DNA oligonucleotides were designed and used:
Donor-1 (D1): 5′-ACTGCTAGAGATTTTCCA-CACTGACTAAAAG-3′
Donor-2 (D2): Biotin-5′-CTTTTAGTCAGTGTGGA-AAATCTCTAGCA-3′
Target-1 (T1): 5′-CTAGAGATTTTCCACACTGACT-AAAAG-3′-Digoxigenin (DIG),
Target-2 (T2): 5′-CTTTTAGTCAGTGTGGAAAA-TCTCTAG-3′-DIG

To form dsDNA, the D1–D2 pair and the T1–T2 pair were mixed in the presence of 0.1 M NaCl and denatured for 10 min at 95°C, followed by an annealing process, gradual cooling down to room temperature. One pmol biotinulated donor dsDNA (D1–D2), 15 pmol IN protein and 5 µl test compounds (100 µM in DMSO) were mixed together in assay buffer (25 mM 3-(N-morpholino)-propanesulfonic acid, pH 7.2, 25 mM NaCl, 10 mM $MgCl_2$, 10 mM DTT, 5% PEG, 10% DMSO), followed by the addition of 0.75 pmol target dsDNA (T1–T2), and adjusted to a final volume of 100 µl and incubated for 1 h at 37°C. After the incubation, the mixture was adjusted to a final volume of 200 µl with ELISA buffer (20 mM Tris [pH 8.0], 0.4 M NaCl, 10 mM EDTA, 0.1 mg/ml sonicated DNA). To harvest the strand-transfer product, the mixture was transferred into a 96-well micro titre plate coated with streptavidin (PIERCE, Rockford, IL, USA), followed by adding an alkaline phosphatase conjugated anti-DIG antibody (Roche Diagnostics, Mannheim, Germany) and a disodium 3-(4-methoxyspiro{1,2-dioxetane-3,2′-(5′-chloro)tricyclo[3.3.1.1^{3,7}]decan}-4-yl) phenyl phosphate (CSPD) substrate (Roche). The lumino-intensity was quantified with a Luminous CT-9000D luminometer (DIA-IATRON, Tokyo, Japan).

In addition to the above two different strand-transfer assays, a strand-transfer assay with radioisotope labelled target DNA and SDS-PAGE was employed in order to visually confirm the strand-transfer inhibition (Craigie *et al.*, 1995). By use of T4 polynucleotide kinase (TAKARA BIO, Osaka, Japan), the 5′ end of 20 mer target oligonucleotide-A (5′-TGTGGAAAATCTCTAGCAGT-3′) was labelled with [γ-^{32}P] ATP (370 MBq/µl, Amersham Bioscience, Tokyo, Japan). After the labelling reaction was terminated by adding EDTA, complementary oligonucleotide-B (5′-ACTGCTAGAGATTTTCCACA-3′) was added, and dsDNA was formed by heat denaturation and gradual cooling to room temperature. Unincorporated [γ-^{32}P]ATP was removed by G-25 Column (Amersham Bioscience, Piscataway, NJ). The reaction products were applied to 20% denatured polyacrylamide gel electrophoresis (300V/25A). The result of the electrophoresis was analysed by BAS-2500 (Fuji film, Tokyo, Japan).

Inhibition kinetics of IN

To analyse the strand-transfer inhibition mechanism of the test compounds, whether the action is competitive inhibition or non-competitive inhibition, Michaelis-Menten constant (K_m) and maximum velocity (V_{max}) were evaluated. Strand-transfer inhibition was evaluated on eight different time points (0, 1, 3, 5, 7.5, 10, 15, and 20 min) with four different compound concentrations (0, 1, 5, 10 µM) and target DNA concentrations (0.167, 0.25, 0.5, and 1 pmol). The initial reaction rate constants of IN were determined by linear regression using linear data points of product concentration–time plots. K_m and V_{max} were calculated from the Y-axis intercept in a plot of the slopes of Lineweaver-Burk analysis.

Intercalative activity evaluation

To clarify the possibility of intercalative activity of test compounds, ethidium bromide (EtBr) displacement assay was carried out following the protocol reported previously (Cain *et al.*, 1978). In brief, 1 µM calf thymus DNA (Invitrogen, Carlsbad, CA, USA) was mixed with EtBr (final concentration at 1.26 µM) and reaction buffer (2 mM HEPES, 10 µM EDTA, 9.4 mM NaCl, pH 7.0), and incubated for 10 min at room temperature. After the incubation, test compounds were added into the calf thymus DNA–EtBr mixture at different concentrations (final concentrations of 0.01–1000 µM). Fluorescence intensity of each mixture was determined by Fluoroskan Ascent FL (Helsinki, Finland. Excited at 544 nm, emitted at 590 nm). Actinomycin D (ICN Biomedical, Aurora, OH, USA), which is known as an intercalator, was employed as the positive control of the assay.

Molecular modelling studies

Molecular modelling studies were carried out using SYBYL software Version 6.9.1 (Tripos, St. Louis, MO, USA) running on an SGI Fuel workstation equipped with 600-MHz R14000 processor (SGI, Mountain View, CA, USA).

Evaluation of *in vitro* antiviral activity.

To evaluate HIV-1 replication inhibition by selected test compounds, *in vitro* antiviral assays were performed using a HeLa4.5/nEGFP reporter cell line. The HeLa4.5/nEGFP reporter cell line was established by transfection of CD4 and LTR driven EGFP reporter protein into the HeLa cell line. HeLa4.5/nEGFP reporter cells were maintained with D-MEM (Sigma) containing 5% FCS (Hyclone, Logan, UT, USA), 500 µg/ml G418, 1 µg/ml blasticidin and 2 µg/ml puromycin.

One day before conducting the assay, 1x10^4 HeLa4.5/nEGFP cells were seeded into clear bottom black 96-well plates (NUNC, Rochester, NY, USA) with

200 μl/well medium and incubated at 37°C, 5% CO_2. The next day, 1250 $TCID_{50}$ HXB2 were added in each well, followed by addition of the test compounds in final concentrations of 5, 1, 0.2, 0.04, 0.008, 0.0016, 0.00032, and 0.000064 μM. Forty-eight hours after infection, the cells were fixed by 3.2% formaldehyde and the nuclei of cells were stained by 10 μg/ml Hoechst33342 (Molecular Probes, Engene, OR, USA). EGFP positive cell number ($EGFP^+$) and Hoechst33342 positive cell number ($hoechst33342^+$) were determined by Cellomics Array Scan, HSC Systems (Beckman Coulter, Tokyo, Japan).

Inhibitory activity of each compound was determined by the following formula:

% inhibition = 1 − {($EGFP^+$ cell number with drug/$hoechst33342^+$ cell number with drug) − ($EGFP^+$ cell number without infection/$hoechst33342^+$ cell number without infection)}/{($EGFP^+$ cell number without drug/$hoechst33342^+$ cell number without drug) − ($EGFP^+$ cell number without infection/$hoechst33342^+$ cell number without infection)}.

Results

A small molecule bearing a carbazole moiety demonstrated strand-transfer inhibitory activity

A diverse library of 12 000 small-molecule compounds was screened for strand-transfer inhibitory activity at 100 μM concentration by M8 apparatus. Seventy-two compounds that demonstrated more than 80% strand-transfer-inhibition were selected and applied to the second screening using in-house strand-transfer assay. In the second screening, to confirm dose-dependent inhibition of the test compounds, each compound was tested at four different concentrations. Of the 72 compounds, a compound bearing a carbazole moiety, 8-chloro-2-[2-(dimethylamino)ethyl]-9-hydroxy-5-methylpyrrolo[3,4-c]carbazole-1,3(2H,6H)-dione (coded as **CA-0**), was found to demonstrate potent strand-transfer inhibitory activity (Figure 1A). As shown in Figure 1B, **CA-0** demonstrated clear dose-dependent inhibition of the strand-transfer reaction with an IC_{50} of 5.00 ±3.31 μM. The dose-dependent inhibition was also confirmed by SDS-PAGE with [γ-^{32}P] labelled target DNA. As demonstrated in Figure 1C, strand-transferred product bands diminished along with increased concentration of the inhibitor. IC_{50} value determined from intensities of the bands was 1.24 ±0.09 μM, which was consistent with that evaluated via the plate assay.

Strand-transfer inhibition of 23 carbazole derivatives, and the relationship between their structures and inhibitory activity

To understand the relationship between structure and strand-transfer inhibition activity, we selected 23 carbazole

Figure 1. Structure and strand transfer inhibitory activity of 8-chloro-2-[2-(dimethylamino) ethyl]-9-hydroxy-5-methylpyrrolo[3,4-c]carbazole-1,3(2H,6H)-dione (**CA-0**)

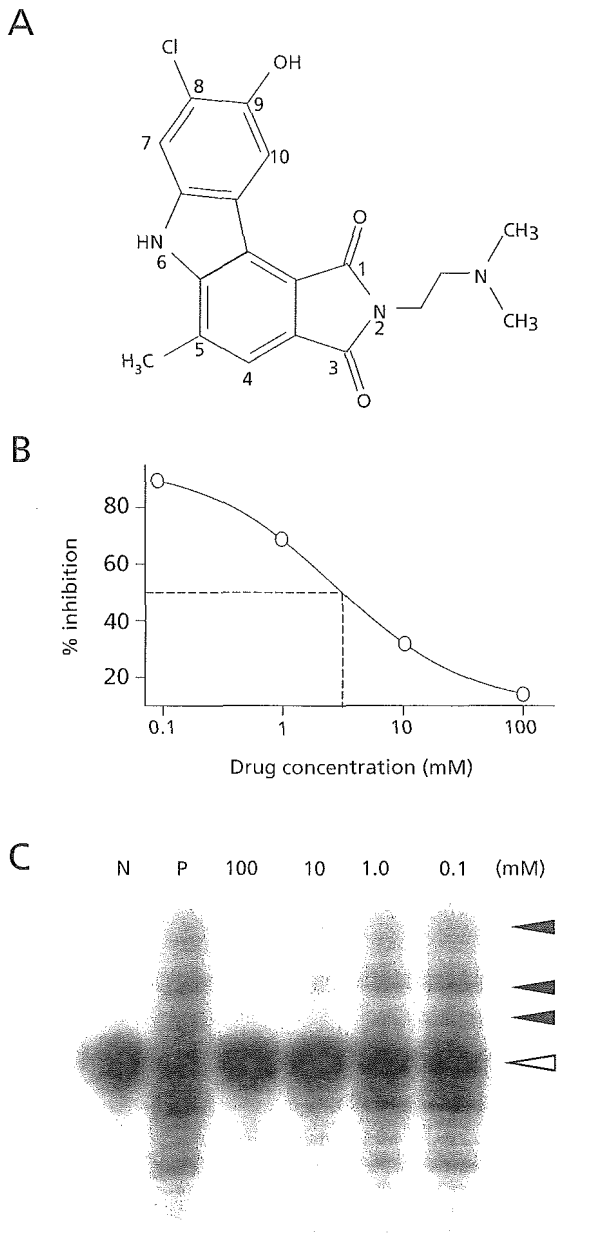

(A) The structure of **CA-0**, a strand transfer inhibitory compound identified from among a library of 12 000 small molecular weight compounds. It has a carbazole structure as a scaffold. The small numbers written beside the structure indicate the residue number of the compound. **(B)** A dose–response curve of **CA-0**. The dotted line indicates the IC_{50} point of the chemical, which was 5.00 ±3.31 μM. **(C)** A strand transfer assay by radioisotope-labelled oligonuceotide. Lane 1 "N" stands for the negative control, with only a radioisotope-labelled nucleotide. Lane 2 "P" stands for positive control, with radioisotope-labelled nucleotide and recombinant integrase. Lanes 3 to 6 were with inhibitor. The open triangle and solid triangle indicate labelled oligonucelotide and strand transfer products, respectively.

derivatives with different substituents. As demonstrated in Figure 2, all compounds had pyrrolo[3,4-c]carbazole structures as scaffolds, and all except **CA-5**, **CA-10** and **CA-19** had 2-dimethylaminoethyl group at position R2. Six of the 23 compounds demonstrated potent strand-transfer inhibition comparable to that of **CA-0**. These compounds were **CA-1**, **CA-4**, **CA-8**, **CA-9**, **CA-12** and **CA-13**. IC_{50} values of these test compounds were similar with positive control S-1360. Moderate inhibitory activities were observed in twelve compounds, **CA-2**, **CA-3**, **CA-7**, **CA-11**, **CA-14**, **CA-15**, **CA-16**, **CA-17**, **CA-18**, **CA-21**, **CA-22** and **CA-23**. Five compounds, **CA-5**, **CA-6**, **CA-10**, **CA-19** and **CA-20**, did not show significant inhibition, even at the highest concentration tested

Figure 2. Structures of **CA-0** and 23 carbazole derivatives evaluated for strand transfer inhibitory activity

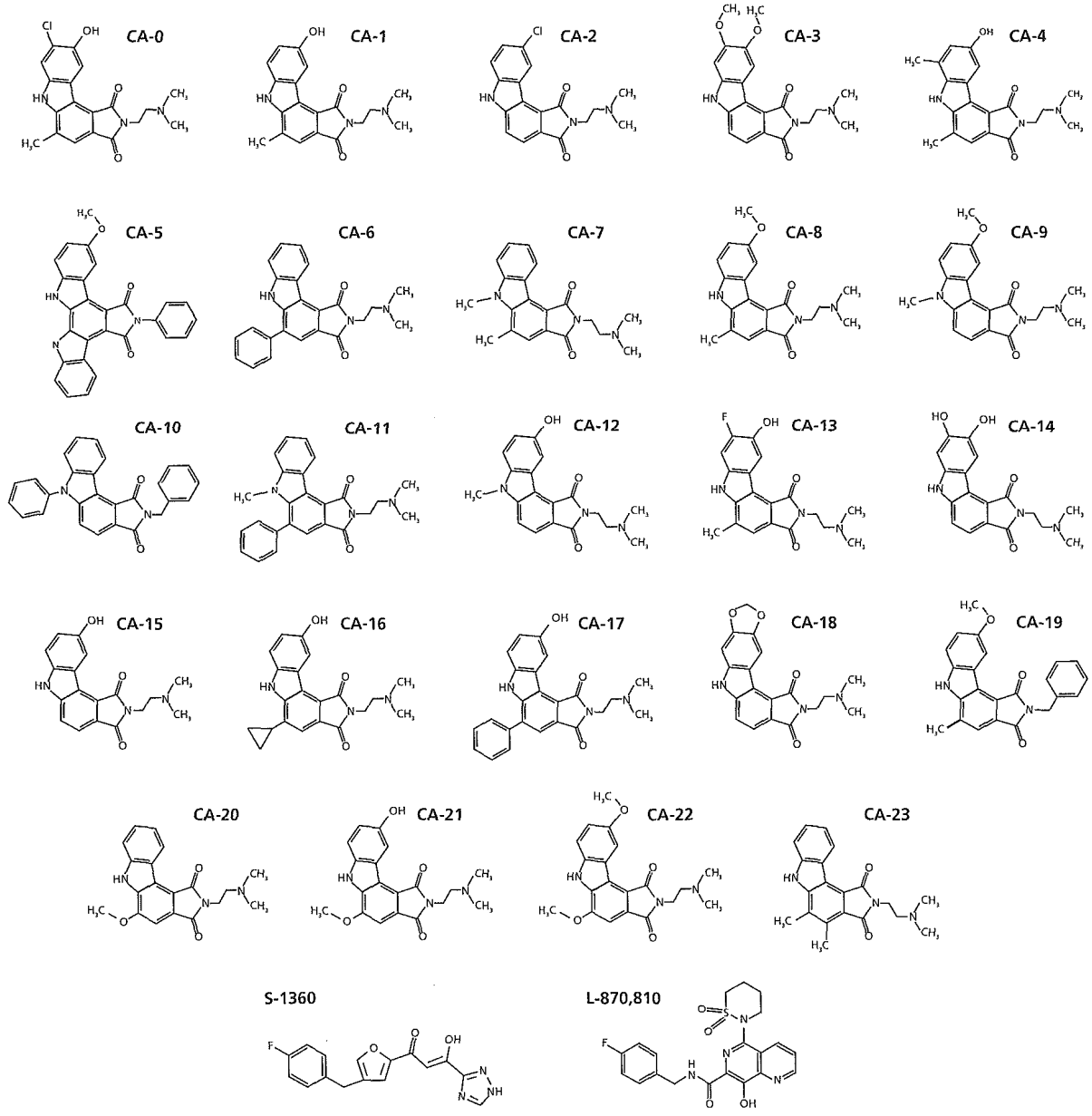

CA-0 and 23 related compounds with carbazole scaffold tested for strand-transfer inhibitory activities are depicted. S-1360 and L-870,810, which have previously been reported as potent IN inhibitors, are also shown.

(100 μM). The compounds that demonstrated potent strand-transfer inhibitory activity were also confirmed by gel-based assay, and IC_{50} values determined from the gel-based assay were consistent with the values determined via in-house plate assay (Table 1).

Carbazole derivatives are competitive inhibitors of integrase

To investigate the strand-transfer inhibitory mechanisms and kinetics of the compounds, we determined V_{max} and K_m of the inhibition by Lineweaver–Burke plot analyses. We selected two compounds, **CA-0** and **CA-13**, for the analyses. As summarized in Table 2, larger K_m values (nM) were observed with higher inhibitory concentration, whereas V_{max} values (RU/min) did not change and remained consistent at any inhibitory concentration (Figure 3). As shown in Figure 3A and 3B, data-fitted lines of different time points converged on the Y axis, indicating that **CA-0** and **CA-13** inhibited strand-transfer in a competitive manner.

Table 1. Strand transfer and *in vitro* viral replication inhibitory activities of carbazole derivatives

	IC_{50} in strand transfer assay		Anti-HIV activity
	Plate assay (μM)	Gel assay (μM)	IC_{50} (μM)
(A) High-inhibitory group			
CA-0	5.00 ±3.31	1.24 ±0.09	0.48 ±0.06
CA-13	4.38 ±2.78	1.13 ±0.21	0.51 ±0.12
CA-1	7.94 ±4.12	2.97 ±0.21	0.92 ±0.15
CA-4	8.99 ±3.39	6.34 ±0.89	1.52 ±0.46
CA-8	6.61 ±4.17	6.38 ±0.32	0.79 ±0.07
CA-9	4.42 ±1.87	4.10 ±0.46	0.80 ±0.11
CA-12	5.93 ±3.53	3.14 ±0.04	0.69 ±0.15
(B) Intermediate-inhibitory group			
CA-2	22.50 ±2.27	ND	ND
CA-3	72.69 ±5.44	ND	ND
CA-7	11.88 ±7.66	ND	ND
CA-11	57.00 ±3.13	ND	ND
CA-14	17.37 ±1.79	ND	ND
CA-15	27.28 ±9.10	ND	ND
CA-16	20.51 ±15.11	ND	ND
CA-17	50.64 ±19.02	ND	ND
CA-18	10.68 ±8.88	ND	ND
CA-21	25.01 ±10.60	ND	ND
CA-22	16.92 ±7.32	ND	ND
CA-23	16.94 ±7.82	ND	ND
(C) Intermediate-inhibitory group			
CA-5	>100	ND	ND
CA-6	>100	ND	ND
CA-10	>100	ND	ND
CA-19	>100	ND	ND
CA-20	>100	ND	ND
(D) Previously reported inhibitor			
S-1360	4.67 ±1.89	ND	ND

Underline, indicates original compound; IC_{50}, 50% inhibition concentration; ND, not done.

Carbazole derivates have not shown intercalative activity

Due to their planar structure and their manner of competitive inhibition, we were concerned that the compounds might have the intercalative activity to destroy substrate dsDNA, rather than binding to the IN to block its enzyme activity. To clear the possibility of the intercalation, EtBr displacement assay was carried out. Since EtBr intercalates into dsDNA and makes visualization possible by growing fluorescence under UV light, intercalative activity of the test compounds can be evaluated by whether the test compounds displace incorporated EtBr out from dsDNA. As shown in Figure 4, fluorescence intensity diminished in a dose-dependent manner by actinomycin D, a compound known as a potent intercalator. In contrast, our two test compounds **CA-0** and **CA-13** did not affect fluorescence intensity, even at the highest concentration of 1 mM, suggesting that **CA-0** and **CA-13** were not intercalators.

Antiviral activity

We employed a single replication infectivity assay using HeLa4.5/EGFP cells to investigate the potency of antiviral activity. IC_{50} values of **CA-0** and the six compounds were 0.48, 0.92, 1.52, 0.79, 0.8, 0.69, 0.51 μM, respectively. The IC_{50} values of all seven compounds were 5.5 to 10.4-fold lower than that of the strand transfer assay (Table 1A). The discrepancy in IC_{50} between the two assays can be explained by stoichiometry of the inhibitor and the target enzyme in the two assays, and the estimated amount of IN in-strand transfer assay was higher than in the

Table 2. Inhibition kinetics of representative carbazole compounds **CA-0** and **CA-13**

Chemical	Concentration	V_{max} (RU/min)	K_m (nM)
CA-0	10 μM	463.16 ±63.16	30.40 ±7.80
	5 μM	402.58 ±32.21	26.21 ±7.40
	1 μM	370.14 ±84.42	12.71 ±2.02
	0 μM	454.55 ±0.02	9.18 ±1.18
CA-13	10 μM	409.70 ±35.47	19.31 ±4.68
	5 μM	439.07 ±164.74	14.83 ±0.24
	1 μM	438.08 ±53.85	11.09 ±2.42
	0 μM	429.83 ±136.46	7.08 ±0.64

Figure 3. Inhibition kinetics assays of two representative carbazole derivatives, **CA-0** and **CA-13**

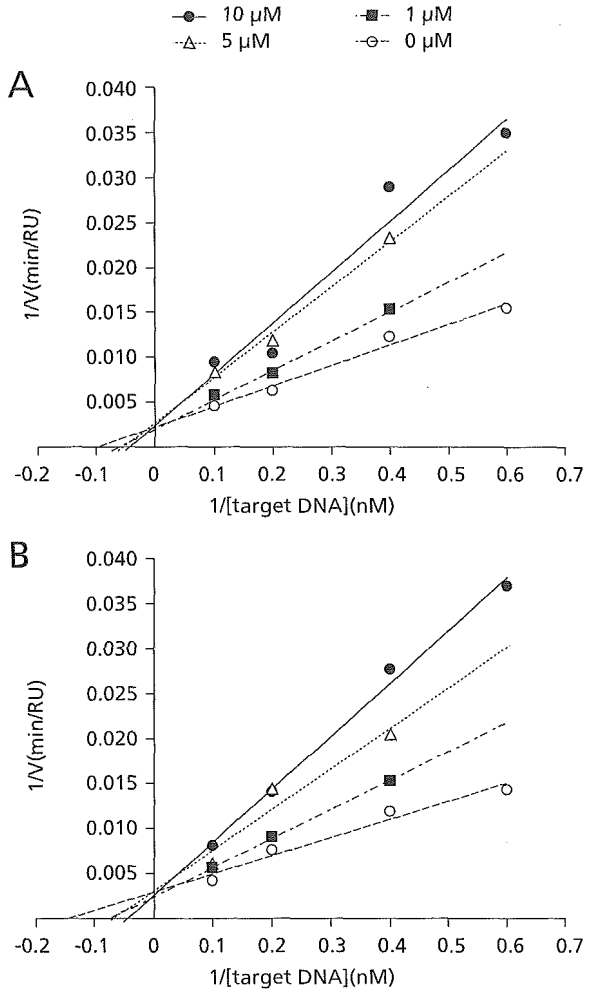

Lineweaver–Burke plot analyses of **(A) CA-0** and **(B) CA-13** are depicted.

Figure 4. Ethidium bromide displacement assays of two representative carbazole derivatives, **CA-0** and **CA-13**

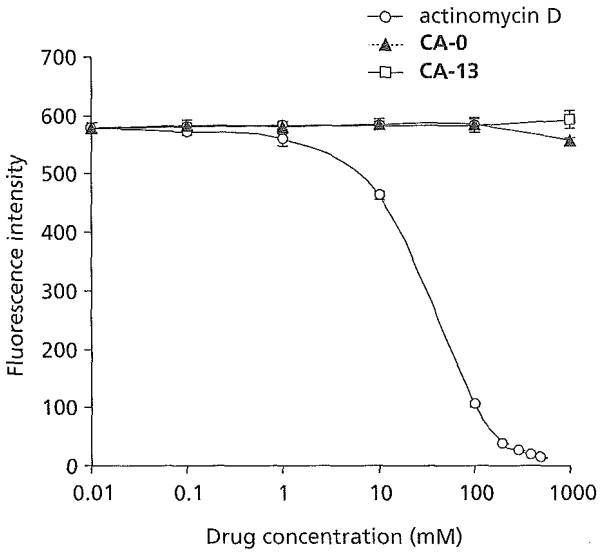

To evaluate intercalative activities of carbazole derivatives, ethidium bromide displacement assays were carried out for two representative compounds, **CA-0** and **CA-13**.

HeLa4.5/EGFP assay. Seven compounds exhibited considerable toxicity, suggesting that efforts toward decreasing toxicity are necessary for the further development of carbazole-based inhibitors.

Discussion

Carbazole, a fused phenyl-ring structure with hydrophobicity, has provided an interesting scaffold for the development of novel drugs. Staurosporine, discovered among microbial alkaloids, was the first carbazole derivative reported to demonstrate biological activity (Omura *et al.*, 1977; Furusaki *et al.*, 1978; Furusaki *et al.*, 1982), which was protein kinase C inhibition (Tamaoki *et al.*, 1986). Other carbazole derivatives have demonstrated various other activities, such as topoisomerase inhibition (Marotto *et al.*, 2002; Facompre *et al.*, 2002; Carrasco *et al.*, 2001), hypotensive activity (Furusaki *et al.*, 1982), platelet aggregation inhibition (Oka *et al.*, 1986), and anti-fungal activity (Sunthitikawinsakul *et al.*, 2003). In this report we present another possible activity of carbazole derivatives, that of HIV-1 integrase inhibitor.

As compounds with three or four fused aromatic ring structures have been reported to demonstrate intercalative activity (Fukui & Tanaka, 1996; Dziegielewski *et al.*, 2002), we initially suspected that our carbazole derivatives also have intercalative activities, penetrating and disturbing target dsDNA, resulting in pseudo strand-transfer inhibition. Indeed, several carbazole derivatives have been recognized to demonstrate intercalative activity (Facompre *et al.*, 2002; Long *et al.*, 2002). We confirmed that actinomycin D, which is a well-known intercalator (Ross *et al.*, 1979; Wilson & Jones, 1982), demonstrated strand-transfer inhibition in our assay (data not shown). However, taking into consideration the data that our carbazole derivatives inhibited strand-transfer in a competitive manner, and also that the compounds could not displace EtBr out from dsDNA, we assume that our derivatives bind to part of the IN molecule, to the region responsible for DNA target

binding or to the catalytic site responsible for strand-transfer activity.

To understand in greater detail the substituents responsible for strand-transfer inhibitory activity, we analysed 23 carbazole derivatives, and classified them into three categories according to their levels of inhibition (Table 1). Six compounds were classified as the high-inhibition group, which demonstrated IC_{50} of less than 10 μM, 12 compounds were classified as the intermediate group, which demonstrated IC_{50} of greater than 10 μM and less than 100 μM, and five compounds were classified as the non-inhibition group, in which we did not observe significant inhibition even at the highest concentration tested (100 μM).

Comparing the compounds between and within these three categories, we recognized three factors responsible for strand-transfer inhibition. The first and most important factor is the incidence of a 2-dimethylaminoethyl group at position R2 (Figure 1A).

CA-8, which possesses a 2-dimethylaminoethyl group at position R2, demonstrated high inhibitory activity (IC_{50}: 6.61 ±4.17 μM), but **CA-19** (IC_{50}: >100 μM), which possesses a phenyl ring structure at the same R2 position, did not demonstrate inhibitory activity. Thus, it is clear that the incidence of a 2-dimethylaminoethyl group, which has a basic property, is critical for strand-transfer inhibition activity. Indeed, we recognized that all compounds in the "high-inhibitory group" and "intermediate-inhibitory group" had this basic substituent at position R2 (Table 1A, 1B, Figure 2). In contrast, three of five compounds in the "non-inhibitory group" had the phenyl ring structure at R2 position. It is thought that these compounds might bind to the acidic region on the IN molecule and compete with the target dsDNA.

The second factor is the incidence of a methyl (Me) group at position R5, R6 or R7. We recognized that compounds in the high inhibitory group had at least one Me group at the R5, R6 or R7 position (Table 1A, Figure 2). Comparing **CA-1** (IC_{50}: 7.94 ±4.12 μM), **CA-4** (IC_{50}: 8.99 ±3.39 μM), and **CA-12** (IC_{50}: 5.93 ±3.53 μM) with **CA-15** (IC_{50}: 27.28 ±9.10 μM), it is clear that the incidence of an Me group within the R5 to R7 positions was an important factor for enhanced inhibitory activity. It seems that the position of the substituent may not be critical between R5 and R6, as we did not see significant differences between **CA-1** (IC_{50}: 7.94 ±4.12 μM) and **CA-12** (IC_{50}: 5.93 ±3.53 μM), and also between **CA-8** (IC_{50}: 6.61 ±4.17 μM) and **CA-9** (IC_{50}: 4.42 ±1.87 μM).

According to the IC_{50} levels of **CA-5** (>100 μM), **CA-6** (>100 μM) and **CA-11** (>100 μM), it appears that bulky substituents at the R5 position have a negative effect on inhibition (Table 1C, Figure 2). Furthermore, the inhibition potential of the three compounds **CA-1** (IC_{50}: 7.94 ±4.12 μM), **CA-16** (IC_{50}: 20.51 ±15.11 μM) and **CA-17** (IC_{50}: 50.64 ±19.02 μM) depended on the molecular size of their R5 substituents. It is probable that the R5 substituents of these compounds were too large and that they interfered with surrounding molecules forming the binding site (Table 1A, 1B, Figure 2). These data indicate that the binding site of carbazole might have a space limitation, and thus the size and shape of the molecules may be important factors for inhibitor activity.

The third factor is the substituent at position R9. Comparing **CA-20** (IC_{50}: >100 μM), **CA-21** (IC_{50}: 25.01 ±10.60 μM) and **CA-22** (IC_{50}: 16.92 ±7.32 μM), these three compounds were identical, with the exception of the substituent at position R9 (Table 1B, 1C, Figure 2). **CA-21** and **CA-22** have hydroxyl residue and a methoxy group at position R9, respectively. We noticed a significant difference in inhibitory activity between **CA-20** and **CA-21**, and between **CA-20** and **CA-22**, suggesting the possibility that both the hydroxyl group and the methoxy group at R9 formed hydrogen bonds with the amino acid molecules forming the binding sites, as these two substituents have the potential to be hydrogen bond acceptors. It appears that hydroxyl and methoxy groups have similar effects on strand-transfer inhibitory activities. In addition to the above three factors, we found that molecular interaction between R8 and R9 substituents, and their arrangement, are also important determinants for efficient inhibitory activity. **CA-3**, with two methoxy groups at R8 and R9, appears to have a bulky arrangement of the two side chains, and demonstrated an IC_{50} of 72.69 ±5.44 μM, whereas **CA-14** and **CA-18**, which were expected to have horizontal arrangements, demonstrated lower IC_{50} values of 17.37 ±1.79 μM and 10.68 ±8.88 μM, respectively (Table 1B, Figure 2).

To summarize these structural elements, and to understand the common structure of molecules that demonstrated strand-transfer inhibitory activity, we superposed inhibitor structures having significant strand-transfer inhibition (**CA-0**, **CA-1**, **CA-4**, **CA-8**, **CA-9**, **CA-12** and **CA-13**) (Figure 5A), and the structures of compounds with no inhibition (**CA-5**, **CA-6**, **CA-10**, **CA-19** and **CA-20**) (Figure 5B). In comparing these two overlapped figures, we found that the compounds with inhibitory activity share a largely identical structure and similar molecular size. In contrast, the non-inhibitory compounds had larger and more uneven-shaped side chains. Overall, the superposed structures indicate that the molecules should be planar and have basic diethylaminoethyl groups to demonstrate strand-transfer inhibitory activity.

In conclusion, we have identified a small molecular weight compound with a carbazole scaffold, which can be the lead compound for developing novel IN inhibitors. Furthermore, analysing the IN inhibitory mechanisms of

Figure 5. A structural comparison between high/intermediate inhibitory compounds and non-inhibitory compounds

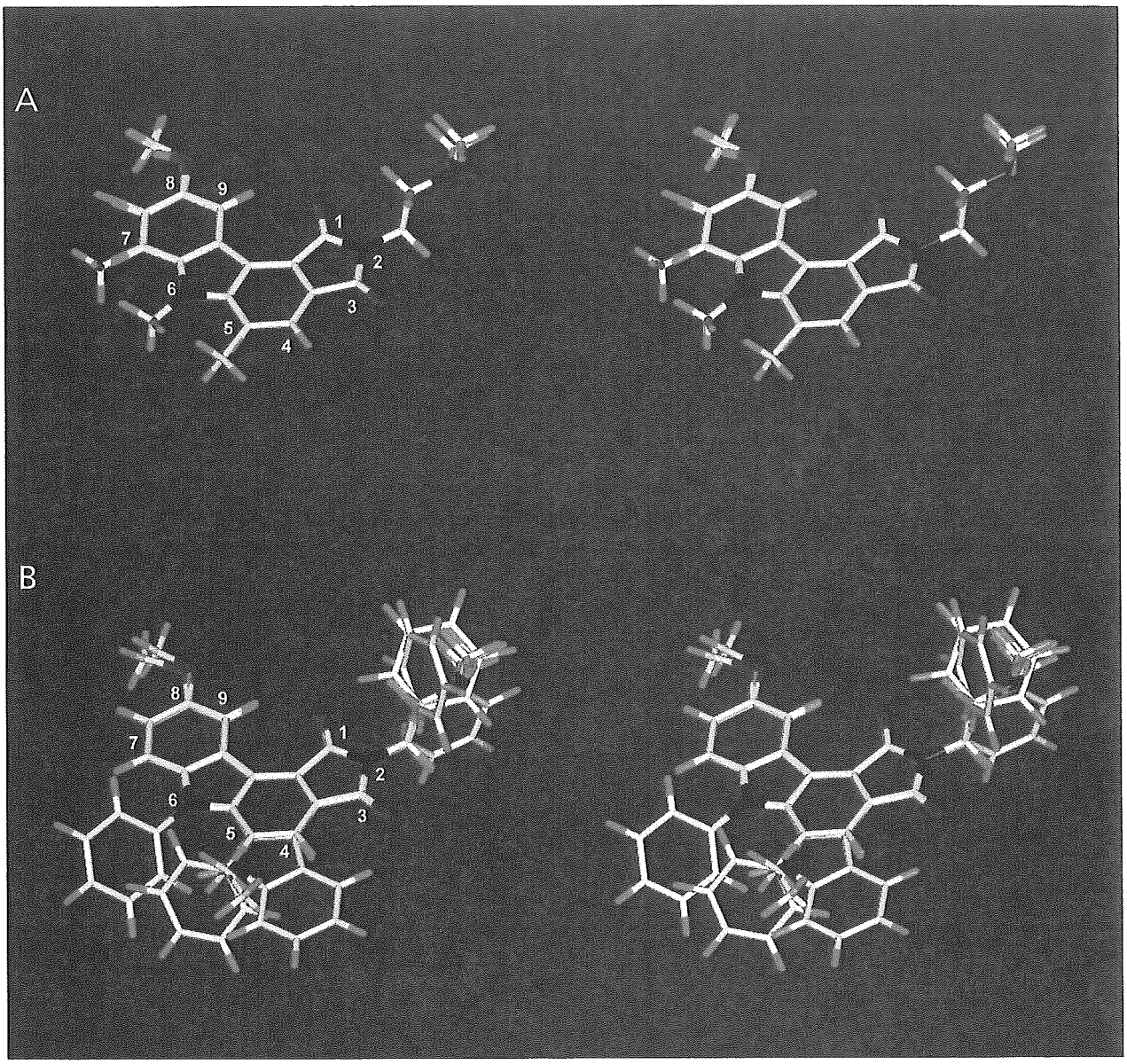

Superposed structures of **(A)** five non-inhibitory compounds, **CA-5**, **6**, **10**, **19** and **20**, and **(B)** seven inhibitory compounds, **CA-0**, **1**, **4**, **8**, **9**, **12** and **13**, are demonstrated in stereo-view images. In both figures, residue numbers are indicated beside the structures. Red, dark blue and light blue indicate oxygen, nitrogen and hydrogen molecules, respectively. Green indicates chlorine or fluorine molecules. SYBYL software Version 6.9.1 running on an SGI Fuel workstation was used to construct the figures.

carbazole derivatives may yield more detailed information regarding HIV-1 IN structure and function.

Acknowledgements

This study was supported by a grant from the Human Sciences Foundation, the Organization of Pharmaceutical Safety and Research of Japan and the Ministry of Health, Labor and Welfare of Japanese Government. This study was partly supported by the Program for Promotion of Fundamental Studies in Health Sciences of the National Institute of Biomedical Innovation (NIBIO)

We would like to thank Dr. Haruo Tanaka and Takuro Shiomi, professor and associate professor of Kitazato

Institute, for their valuable advice and comments. We would also like to thank the laboratory members of Toyama Chemical Co. Ltd. for supplying the compounds in the study. Finally, we would like to thank Ms. Mary Phillips and Ms. Yumi Fujiuji for preparing the manuscript.

References

Balzarini J (2004) Current status of the non-nucleoside reverse transcriptase inhibitors of human immunodeficiency virus type 1. *Current Topics in Medicinal Chemistry* **4**:921–944.

Burke CJ, Sanyal G, Bruner MW, Ryan JA, LaFemina RL, Robbins HL, Zeft AS, Middaugh CR & Cordingley MG (1992) Structural implications of spectroscopic characterization of a putative zinc finger peptide from HIV-1 integrase. *The Journal of Biological Chemistry* **267**:9639–9644.

Cain BF, Baguley BC & Denny WA (1978) Potential antitumor agent. 28. deoxyribonucleic acid polyintercalating agents. *Journal of Medicinal Chemistry* **21**:658–668.

Carrasco C, Vezin H, Wilson WD, Ren J, Chaires JB & Bailly C (2001) DNA binding properties of the indolocarbazole antitumor drug NB-506. *Anticancer Drug Design* **16**:99–107.

Chun TW, Finzi D, Margolick J, Chadwick K, Schwartz D & Siliciano RF (1995) *In vivo* fate of HIV-1-infected T cells: quantitative analysis of the transition to stable latency. *Nature Medicine* **1**:1284–1290.

Craigie R, Hickman AB & Engelman A (1995) Integrase. in *HIV: A Practical Approach – Volume 2: Biochemistry, Molecular Biology, and Drug Discovery*; pp. 53–71. Edited by J Karn. New York: Oxford University Press.

Dayam R & Neamati N (2003) Small-molecule HIV-1 integrase inhibitors: the 2001–2002 update. *Current Pharmacology Design* **9**:1789–1802.

De Clercq E (1992) HIV inhibitors targeted at the reverse transcriptase. *AIDS Research and Human Retroviruses* **8**:119–134.

Dziegielewski J, Slusarski B, Konitz A, Skladanowski A & Konopa J (2002) Intercalation of imidazoacridinones to DNA and its relevance to cytotoxic and antitumor activity. *Biochemical Pharmacology* **63**:1653–1662.

Engelman A & Craigie R (1992) Identification of conserved amino acid residues critical for human immunodeficiency virus type 1 integrase function *in vitro*. *Journal of Virology* **66**:6361–6369.

Engelman A, Englund G, Orenstein JM, Martin MA & Craigie R (1995) Multiple effects of mutations in human immunodeficiency virus type 1 integrase on viral replication. *Journal of Virology* **69**:2729–2736.

Engelman A, Hickman AB & Craigie R (1994) The core and carboxyl-terminal domains of the integrase protein of human immunodeficiency virus type 1 each contribute to nonspecific DNA binding. *Journal of Virology* **68**:5911–5917.

Facompre M, Carrasco C, Colson P, Houssier C, Chisholm JD, Van Vranken DL & Bailly C (2002) DNA binding and topoisomerase I poisoning activities of novel disaccharide indolocarbazoles. *Molecular Pharmacology* **62**:1215–1227.

Fukui K & Tanaka K (1996) The acridine ring selectively intercalated into a DNA helix at various types of abasic sites: double strand formation and photophysical properties. *Nucleic Acids Research* **24**:3962–3967.

Furusaki A, Hashiba N, Matsumoto T, Hirano A, Iwai Y & Omura S (1978) X-ray crystal structure of staurosporine: a new alkaloid from a Streptomyces strains. *Journal of the Chemical Society. Chemical Communications* 800–801.

Furusaki A, Hashiba N, Matsumoto T, Hirano A, Iwai Y & Omura S (1982) The crystal and molecular structure of staurosporine, a new alkaloid from a Streptomyces strains. *Bulletin of the Chemical Society of Japan* **55**:3681–3685.

Goldgur Y, Craigie R, Cohen GH, Fujiwara T, Yoshinaga T, Fujishita T, Sugimoto H, Endo T, Murai H & Davies DR (1999) Structure of the HIV-1 integrase catalytic domain complexed with an inhibitor: a platform for antiviral drug design. *Proceedings of the National Academy of Sciences, USA* **96**:13040–13043.

Grobler JA, Stillmock K, Hu B, Witmer M, Felock P, Espeseth AS, Wolfe A, Egbertson M, Bourgeois M, Melamed J, Wai JS, Young S, Vacca J & Hazuda DJ (2002) Diketo acid inhibitor mechanism and HIV-1 integrase: implications for metal binding in the active site of phosphotransferase enzymes. *Proceedings of the National Academy of Sciences USA* **99**:6661–6666.

Hazuda DJ, Anthony NJ, Gomez RP, Jolly SM, Wai JS, Zhuang L, Fisher TE, Embrey M, Guare JP, Jr., Egbertson MS, Vacca JP, Huff JR, Felock PJ, Witmer MV, Stillmock KA, Danovich R, Grobler J, Miller MD, Espeseth AS, Jin L, Chen IW, Lin JH, Kassahun K, Ellis JD, Wong BK, Xu W, Pearson PG, Schleif WA, Cortese R, Emini E, Summa V, Holloway MK & Young SD (2004) A naphthyridine carboxamide provides evidence for discordant resistance between mechanistically identical inhibitors of HIV-1 integrase. *Proceedings of the National Academy of Sciences USA* **101**:11233–11238.

Hazuda DJ, Felock P, Witmer M, Wolfe A, Stillmock K, Grobler JA, Espeseth A, Gabryelski L, Schleif W, Blau C & Miller MD (2000) Inhibitors of strand transfer that prevent integration and inhibit HIV-1 replication in cells. *Science* **287**:646–650.

Imamichi T (2004) Action of anti-HIV drugs and resistance: reverse transcriptase inhibitors and protease inhibitors. *Current Pharmaceutical Design* **10**:4039–4053.

Johnson AA, Marchand C & Pommier Y (2004) HIV-1 integrase inhibitors: a decade of research and two drugs in clinical trial. *Current Topics in Medicinal Chemistry* **4**:1059–1077.

Khan E, Mack JP, Katz RA, Kulkosky J & Skalka AM (1991) Retroviral integrase domains: DNA binding and the recognition of LTR sequences. *Nucleic Acids Research* **19**:851–860.

Kohl NE, Emini EA, Schleif WA, Davis LJ, Heimbach JC, Dixon RA, Scolnick EM & Sigal IS (1988) Active human immunodeficiency virus protease is required for viral infectivity. *Proceedings of National Academy of Sciences USA* **85**:4686–4690.

LaFemina RL, Schneider CL, Robbins HL, Callahan PL, LeGrow K, Roth E, Schleif WA & Emini EA (1992) Requirement of active human immunodeficiency virus type 1 integrase enzyme for productive infection of human T-lymphoid cells. *Journal of Virology* **66**:7414–7419.

Long BH, Rose WC, Vyas DM, Matson JA & Forenza S (2002) Discovery of antitumor indolocarbazoles: rebeccamycin, NSC 655649, and fluoroindolocarbazoles. *Current Medicinal Chemistry. Anti-Cancer Agents* **2**:255–266.

Marotto A, Kim YS, Schulze E & Pindur U (2002) New indolocarbazoles as antitumour active compounds: evaluation of the target by experimental and theoretical studies. *Pharmazie* **57**:194–197.

Oka S, Kodama M, Takeda H, Tomizuka N & Suzuki H (1986) Staurosporine, a potent platelet aggregation inhibitor form a *Streptomyces* species. *Agricultural and Biological Chemistry* **50**:2723–2727.

Omura S, Iwai Y, Hirano A, Nakagawa A, Awaya J, Tsuchya H, Takahashi Y & Masuma R (1977) A new alkaloid AM-2282 of *Streptomyces* origin. Taxonomy, fermentation, isolation and preliminary characterization. *The Journal of Antibiotics (Tokyo)* **30**:275–282.

Pluymers W, Pais G, Van Maele B, Pannecouque C, Fikkert V, Burke TR, Jr., De Clercq E, Witvrouw M, Neamati N & Debyser Z (2002) Inhibition of human immunodeficiency virus type 1 integration by diketo derivatives. *Antimicrobial Agents and Chemotherapy* **46**:3292–3297.

Pommier Y, Marchand C & Neamati N (2000) Retroviral integrase inhibitors year 2000: update and perspectives. *Antiviral Research* **47**:139–148.

Ross WE, Glaubiger D & Kohn KW (1979) Qualitative and quantitative aspects of intercalator-induced DNA strand breaks. *Biochimica et Biophyssica Acta* **562**:41–50.

Ruscetti FW (1985) Immunopathology associated with human lymphotropic retroviruses. *Survey and Synthesis of Pathology Research* **4**:216–226.

Schauer M & Billich A (1992) The N-terminal region of HIV-1 integrase is required for integration activity, but not for DNA-binding. *Biochemical and Biophysical Research Communications* **185**:874–880.

Sunthitikawinsakul A, Kongkathip N, Kongkathip B, Phonnakhu S, Daly JW, Spande TF, Nimit Y & Rochanaruangrai S (2003) Coumarins and carbazoles from *Clausena excavata* exhibited antimycobacterial and antifungal activities. *Planta Medica* **69**:155–157.

Tamaoki T, Nomoto H, Takahashi I, Kato Y, Morimoto M & Tomita F (1986) Staurosporine, a potent inhibitor of phospholipid/Ca^{++} dependent protein kinase. *Biochemical and Biophysical Research Communications* **135**:397–402.

Tronchet JM & Seman M (2003) Non-nucleoside inhibitors of HIV-1 reverse transcriptase: from the biology of reverse transcription to molecular design. *Current Topics in Medicinal Chemistry* **3**:1496–1511.

Wilson WD & Jones RL (1982) Interaction of actinomycin D, ethidium, quinacrine, daunorubicin, and tetralysine with DNA: 31P NMR chemical shift and relaxation investigation. *Nucleic Acids Research* **10**:1399–1410.

Woerner AM & Marcus-Sekura CJ (1993) Characterization of a DNA binding domain in the C-terminus of HIV-1 integrase by deletion mutagenesis. *Nucleic Acids Research* **21**:3507–3511.

Received 22 August 2005, accepted 27 September 2005

Stereoselective Synthesis of [L-Arg-L/D-3-(2-naphthyl)alanine]-Type (*E*)-Alkene Dipeptide Isosteres and Its Application to the Synthesis and Biological Evaluation of Pseudopeptide Analogues of the CXCR4 Antagonist FC131

Hirokazu Tamamura,*,† Kenichi Hiramatsu,† Satoshi Ueda,† Zixuan Wang,‡ Shuichi Kusano,§ Shigemi Terakubo,§ John O. Trent,∥ Stephen C. Peiper,‡ Naoki Yamamoto,⊥ Hideki Nakashima,§ Akira Otaka,† and Nobutaka Fujii*,†

Graduate School of Pharmaceutical Sciences, Kyoto University, Sakyo-ku, Kyoto 606-8501, Japan, Medical College of Georgia, Augusta, Georgia 30912, St. Marianna University, School of Medicine, Miyamae-ku, Kawasaki 216-8511, Japan, James Graham Brown Cancer Center, University of Louisville, Louisville, Kentucky 40202, and Tokyo Medical and Dental University, School of Medicine, Bunkyo-ku, Tokyo 113-8519, Japan

Received July 18, 2004

L,L-Type and L,D-type (*E*)-alkene dipeptide isosteres (EADIs) that have unnatural side chains at the α-position were synthesized by the combination of stereoselective aziridinyl ring-opening reactions and organozinc−copper-mediated *anti*-S_N2' reactions toward a single substrate of γ,δ-*cis*-γ,δ-epimino (*E*)-α,β-enoate. The utility of this methodology was demonstrated by the stereoselective synthesis of a set of diastereomeric EADIs of L-Arg-L/D-3-(2-naphthyl)alanine (Nal) that is contained in a small CXCR4 antagonist FC131 [*cyclo*(-D-Tyr-Arg-Arg-Nal-Gly-)]. Furthermore, a (Nal-Gly)-type EADI was synthesized by samarium diiodide (SmI_2)-induced reduction of a γ-acetoxy-α,β-enoate. Several FC131 analogues, in which these EADIs were inserted for reduction of their peptide character, were synthesized with analogues containing reduced amide-type dipeptide isosteres to investigate the importance of these amide bonds for anti-HIV and CXCR4-antagonistic activity.

Introduction

The practical utility of (*E*)-alkene dipeptide isosteres (EADIs) has been intensively investigated in structure−activity relationship (SAR) studies of biologically active peptides toward development of peptide-lead drugs.[1−7] Backbone replacements of amide bonds in peptides by EADIs provide information on the contributions of the corresponding amide bonds on biological activity. We previously established a completely stereocontrolled synthetic process for L,L-type and L,D-type EADIs starting from L-amino acid.[8,9] As shown in Scheme 1, treatment of *N*-aryl-γ,δ-*cis*-γ,δ-epimino (*E*)-α,β-enoates (*cis*-(*E*)-enoates) **1** with methanesulfonic acid (MSA) gives γ-mesyloxy-α,β-enoates **2**, which can be converted into L,D-type EADIs **3** by organocopper-mediated α-alkylation via *anti*-S_N2' reactions, whereas organocopper treatment of *cis*-(*E*)-enoates **1** affords L,L-type EADIs **4**. However, this synthetic procedure has not yet been optimized, because it involves a potential limitation on the introduction of functional groups into the side chain (R^3) at the α-position. In a standard procedure, organocopper reagents, which were prepared by CuCN and RLi or RMgX (X = Cl or Br), are used for α-alkylation.[2,4] In the α-alkylation of the synthesis of (Xaa-L/D-Glu)-type EADIs,[10] organozinc−copper reagents are used, which are prepared from $IZnCH_2CH_2CO_2R$ and CuCN.[11−15] In this study, to demonstrate the general utility of organozinc−copper reagents, a set of EADIs of L-Arg-L/D-3-(2-naphthyl)alanine (Nal) were synthesized as model compounds via the γ,δ-*cis*-γ,δ-epimino (*E*)-α,β-enoate by the combination of MSA-mediated aziridinyl ring-opening reactions and α-alkylation with organozinc−copper reagents, which were prepared from 2-naphthylmethylZnBr and CuCN. The dipeptide sequence, Arg-Nal, is part of the low molecular weight CXCR4 antagonist, FC131, which was recently developed by us (Figure 1).[16]

Scheme 1[a]

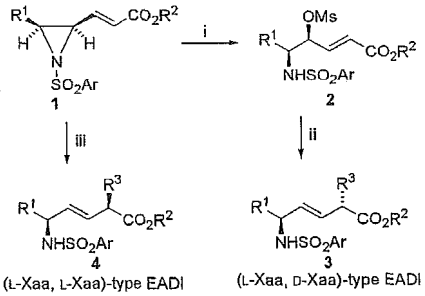

[a] R^1, R^2, R^3 = alkyl; Ar = 2,4,6-trimethylphenylsulfonyl (Mts) or Ts. Reagents: (i) MsOH; (ii) $R^3Cu(CN)MgX{\cdot}BF_3$ (X = Cl or Br) or $R^3Cu(CN)Li{\cdot}BF_3$; (iii) $R^3Cu(CN)MgX{\cdot}2LiX$ (X = Cl or Br) or $R^3Cu(CN)Li{\cdot}2LiX$.

CXCR4 is a chemokine receptor, which is involved in cell progression and metastasis of several types of cancer,[17−19] HIV entry,[20] and rheumatoid arthritis.[21,22] Thus, several inhibitors directed against CXCR4 have been developed.[23−27] We previously found a highly potent CXCR4 antagonist, T140, which is a 14-mer

* Corresponding authors. Tel: +81 75 753 4551, Fax: +81 75 753 4570, E-mail: tamamura@pharm.kyoto-u.ac.jp; nfujii@pharm.kyoto-u.ac.jp.
† Kyoto University.
‡ Medical College of Georgia.
§ St. Marianna University.
∥ University of Louisville.
⊥ Tokyo Medical and Dental University.

10.1021/jm049429h CCC: $30.25
Published on Web 12/21/2004

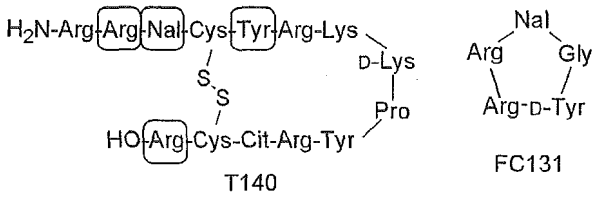

Figure 1. Structures of T140 and its downsized peptide FC131. Circled residues are the indispensable residues of T140 for the expression of strong CXCR4-antagonistic activity. Nal = L-3-(2-naphthyl)alanine, Cit = L-citrulline.

peptide with a disulfide bridge, and we identified four critical residues: Arg^2, Nal^3, Tyr^5, and Arg^{14} (Figure 1).[28-30] Molecular-size reduction of T140 based on the structural requirement led to the discovery of FC131, which has a cyclic pentapeptide template,[31-37] with CXCR4-antagonistic and anti-HIV activity comparable to those of T140.[16] We wish to investigate contributions of each amide bond in FC131 to the biological activity in order to develop pseudopeptides, in which the peptide character is reduced to obtain more druglike structures. For this purpose, EADIs and reduced amide-type dipeptide isosteres (RADIs) of Arg-Nal and Nal-Gly are required, because the amide bonds between Arg^2 and Nal^3 and between Nal^3 and Cys^4 were found to be cleaved by treatment of T140 analogues with rat liver homogenates.[36,39] Thus, (L-Arg-L/D-Nal)-type EADIs were synthesized in the study described here, and a (Nal-Gly)-type EADI was also synthesized by another method using the samarium diiodide (SmI_2)-induced reduction of a γ-acetoxy-α,β-enoate.[40,41] RADIs of Arg-Nal and Nal-Gly were prepared by a standard method of reductive amination. Then, several FC131 analogues, in which the above isosteres were introduced, were synthesized to identify the biological importance of these amide bonds.

Results and Discussion

Synthesis of (L-Arg-L/D-Nal)-Type EADIs. (L-Arg-L/D-Nal)-type EADIs were synthesized via the same key intermediate *N*-2-nitrobenzenesulfonyl (Ns)-γ,δ-*cis*-γ,δ-epimino (*E*)-α,β-enoate, **9**, as synthetic model compounds for the investigation of the feasibility of α-alkylation using organozinc−copper reagents as well as precursor dipeptide isosteres used for the synthesis of partial nonpeptide analogues of FC131 (Scheme 2). Boc-Arg(Mts)-OMe (Mts = 2,4,6-trimethylbenzenesulfonyl) **5** was treated successively with diisobutylaluminum hydride (DIBAL-H) and vinylmagnesium chloride (CH_2=$CHMgCl$) to give exclusively the *threo*-amino alcohol **6** (a separable mixture of allyl alcohol **6**/*erythro*-isomer of **6** = 12:1). N^{α}-Ns protection[42,43] after the cleavage of the N^{α}-Boc group of **6** with HCl/dioxane followed by successive treatments consisting of the Mitsunobu reaction,[44] ozonolysis, and the modified Horner−Wadsworth−Emmons olefination[45] afforded *cis*-(*E*)-enoate **9**. *Anti*-S_N2' reaction of **9** with an organozinc−copper reagent,[11-15] 2-naphthylmethylCu(CN)-ZnBr·2LiCl, afforded an L,L-type EADI **10**, in which a (2*R*)-2-naphthylmethyl side chain was incorporated at the α-position, stereoselectively in 83% yield (diastereoselection > 99:1 from NMR analysis). N^{α}-Fmoc substitution for the N^{α}-Ns group of **10** followed by selective deprotection of the benzyl ester using thioanisole/TFA afforded a desired EADI, Fmoc-L-Arg(Mts)-ψ[(*E*)-CH=CH]-L-Nal-OH, **12**. Alternatively, exposure of **9** to MSA/$CHCl_3$ afforded exclusively δ-aminated γ-mesyloxy-α,β-enoate **13** by regio- and stereoselective S_N2 ring-opening reaction at the γ-carbon of **9**. Mesylate **13** was successively treated by an organozinc−copper reagent, 2-naphthylmethylCu(CN)ZnBr·BF_3, to afford an L,D-type EADI **14**, in which a (2*S*)-2-naphthylmethyl side chain was incorporated at the α-position, stereoselectively via an *anti*-S_N2'mechanism in 67% yield (diastereoselection > 99:1 from NMR analysis). **14** was similarly converted into another desired EADI, Fmoc-L-Arg(Mts)-ψ[(*E*)-CH=CH]-D-Nal-OH, **16**. As such, α-alkylation of both a *cis*-(*E*)-enoate and its ring-opened product using organozinc−copper reagents was successfully performed in the synthesis of (L-Arg-L/D-Nal)-type EADIs. An *N*-Ns group could be used in this synthetic scheme as an orthogonal *N*-protecting (activating) group instead of an *N*-Mts or *N*-Ts group. Relative configurations of the allyl alcohols (**6** and its erythro isomer) were determined by comparative nuclear Overhauser effect (NOE) measurements of these oxazolidinone derivatives **17** and **18** (Scheme 2).[2] The (*E*)-geometry of the double bond in the synthesized EADIs was assigned based on the coupling constant of the two olefinic protons on ^1H NMR analysis.

Synthesis of (L-Nal-Gly)-Type EADI. An (L-Nal-Gly)-type EADI was synthesized as shown in Scheme 3. Boc-L-Nal-OMe **19** was treated sequentially with DIBAL-H and CH_2=$CHMgCl$ to give a diastereomixture of allyl alcohol **20**. Acetylation of **20** followed by ozonolysis and the modified Horner−Wadsworth−Emmons olefination afforded a γ-acetoxy-α,β-unsaturated ester **22**. Acetate **22** was reduced with SmI_2−^{t}BuOH to yield an (L-Nal-Gly)-type EADI **23** in 95% yield,[40,41] followed by deprotection of the N^{α}-Boc group and *tert*-butyl ester with TFA and reprotection with an N^{α}-Fmoc group to afford the desired EADI, Fmoc-L-Nal-ψ[(*E*)-CH=CH]-Gly-OH, **24**.

Synthesis of RADIs of Arg-Nal and Nal-Gly. (L-Arg-L-Nal)- and (L-Nal-Gly)-type RADIs were prepared for comparative studies. As shown in Scheme 4, Arg- and Nal-derived Weinreb amides **25** and **29** were treated with DIBAL-H to afford the corresponding aldehyde derivatives. Subsequently, reductive amination of the aldehydes was performed by treatments with carboxy-protected amino acids in the presence of acetic acid and sodium triacetoxy borohydride [$NaBH(OAc)_3$] to afford secondary amines **26** and **30**, respectively.[46] Protection of the *sec*-amino groups with Cbz groups followed by deprotection of the N^{α}-Boc group and *tert*-butyl ester with TFA and reprotection with an N^{α}-Fmoc group afforded the desired RADIs, Fmoc-L-Arg(Mts)-ψ-[CH_2−N(Cbz)]-L-Nal-OH, **28**, and Fmoc-L-Nal-ψ[CH_2−N(Cbz)]-Gly-OH, **32**, respectively.

Synthesis of Cyclic Pseudopeptides. The protected peptide chains were constructed on a hydrazino resin **34** by Fmoc-based solid-phase synthesis using ^{t}Bu and 2,2,4,6,7-pentamethyldihydrobenzofuran-5-sulfonyl (Pbf) groups for side-chain protection of D-Tyr and Arg, respectively (Scheme 5). N^{α}-Fmoc-protected dipeptide isosteres, EADIs **12**, **16**, and **24** and RADIs **28** and **32**, were similarly condensed. In the synthesis of cyclic pseudopeptides, two steps of deprotection/cleavage were adopted to prevent guanidino groups of Arg from

Scheme 2[a]

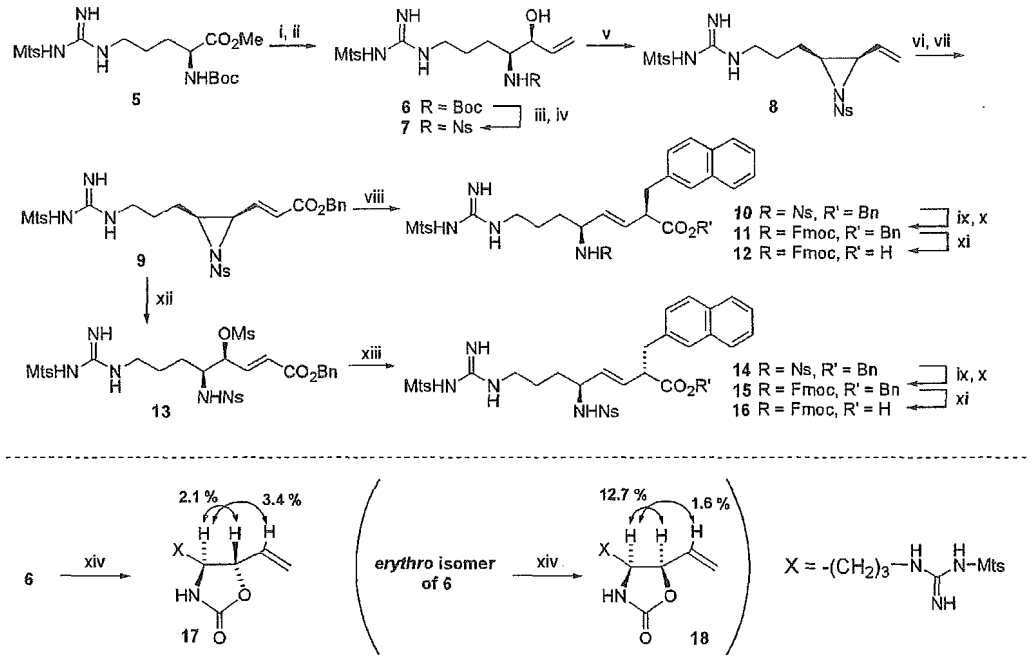

[a] Reagents: (i) DIBAL-H; (ii) CH_2=CHMgCl; (iii) HCl, anisole; (iv) Ns-Cl, pyridine; (v) Ph_3P, DEAD; (vi) O_3, then Me_2S; (vii) $(EtO)_2P(O)CH_2CO_2Bn$, LiCl, DIPEA; (viii) 2-naphthylmethylCu(CN)ZnBr·2LiCl; (ix) PhSH, K_2CO_3; (x) Fmoc-OSu, Et_3N; (xi) thioanisole, TFA; (xii) MsOH; (xiii) 2-naphthylmethylCu(CN)ZnBr·BF_3; (xiv) NaH.

Scheme 3[a]

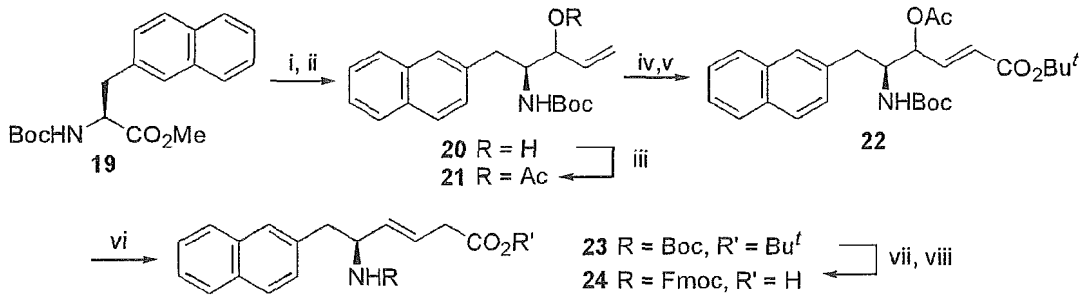

[a] Reagents: (i) DIBAL-H; (ii) CH_2=CHMgCl; (iii) Ac_2O, DMAP, pyridine; (iv) O_3, then Me_2S; (v) $(EtO)_2P(O)CH_2CO_2{}^tBu$, LiCl, DIPEA; (vi) SmI_2, ^tBuOH; (vii) anisole, TFA; (viii) Fmoc-OSu, Et_3N.

Scheme 4[a]

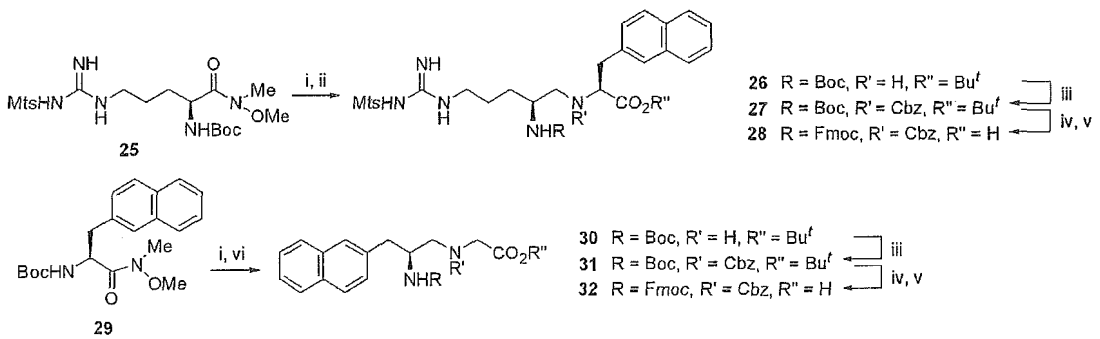

[a] Reagents: (i) DIBAL-H; (ii) H-Nal-O^{t}Bu, AcOH, $NaBH(OAc)_3$; (iii) Cbz-Cl, Et_3N; (iv) anisole, TFA; (v) Fmoc-OSu, Et_3N; (vi) H-Gly-O^{t}Bu, AcOH, $NaBH(OAc)_3$.

participating in cyclizing reaction as follows. After construction of peptide chains, pseudopeptide hydrazides **36** were obtained by cleavage from the resin **35** using 10% TFA/$CHCl_3$ without cleavage of Pbf, Mts, and Cbz groups (first deprotection). Cyclization of linear pseudopeptides by the azide procedure[47] in highly

Scheme 5[a]

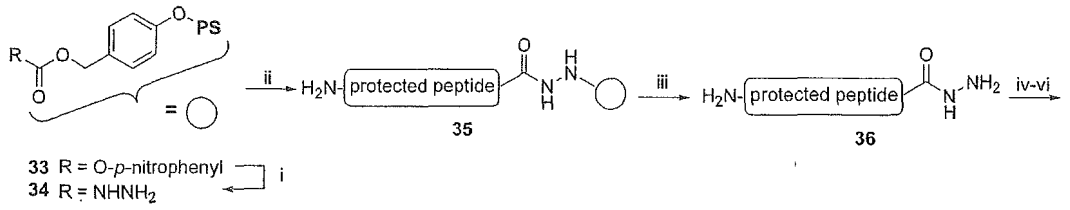

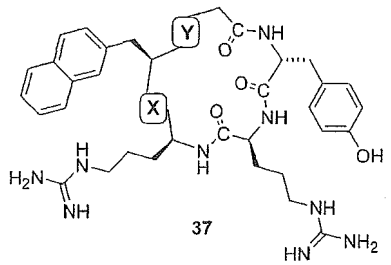

Compd.	Sequence (*cyclo*)	X	Y
FC131	(-D-Tyr-Arg-Arg-Nal-Gly-)	-CO-NH-	-CO-NH-
37a	(-D-Tyr-Arg-Arg-Nal-Gly-)	-CH=CH-	-CO-NH-
37b	(-D-Tyr-Arg-Arg-Nal-Gly-)	$-CH_2$-NH-	-CO-NH-
37c	(-D-Tyr-Arg-Arg-Nal-Gly-)	-CO-NH-	-CH=CH-
37d	(-D-Tyr-Arg-Arg-Nal-Gly-)	-CO-NH-	$-CH_2$-NH-
37e	(-D-Tyr-Arg-Arg-D-Nal-Gly-)	-CO-NH-	-CO-NH-
37f	(-D-Tyr-Arg-Arg-D-Nal-Gly-)	-CH=CH-	-CO-NH-

[a] Reagents: (i) $NH_2NH_2 \cdot H_2O$; (ii) Fmoc-based SPPS; (iii) TFA; (iv) HCl, isoamyl nitrite; (v) DIPEA; (vi) 1 M TMSBr–thioanisole/TFA, *m*-cresol, 1,2-ethanedithiol.

Table 1. Activity and Cytotoxicity of the Synthetic Compounds

compound (no.)	CC_{50}[a] (μM)	EC_{50}[b] (μM)	IC_{50}[c] (μM)
FC131	> 100	0.073	0.0045 ± 0.0018
37a	> 100	2.4	31–100[d]
37b	> 100	> 100	> 100
37c	> 100	2.4	0.18 ± 0.10
37d	> 100	0.98	0.032 ± 0.011
37e	> 100	1.9	0.19 ± 0.071
37f	> 100	9.1	21
T140	> 10	0.035	0.0039 ± 0.0004
AZT	57	0.018	

[a] CC_{50} values are based on the reduction of the viability of mock-infected MT-4 cells. Because the cytotoxicity of T140 was previously evaluated as CC_{50} > 40 μM, further estimation at high concentrations was omitted in this study. [b] EC_{50} values are based on the inhibition of HIV-induced cytopathogenicity in MT-4 cells. [c] IC_{50} values are based on the inhibition of [^{125}I]-SDF-1-binding to CXCR4 transfectants of CHO cells. All data are the mean values for at least three independent experiments. [d] **37a** showed significant antagonistic activity in 100 μM but hardly showed activity in 31 μM.

diluted dimethylformamide (DMF) solution followed by deprotection of Pbf, Mts, and Cbz groups with 1 M TMSBr–thioanisole/TFA (second deprotection) gave the desired cyclic pseudopeptides **37**.

Biological and Conformational Evaluation of Synthetic Cyclic Pseudopeptides. Anti-HIV activity based on the inhibition of HIV-1-induced cytopathogenicity in MT-4 cells was evaluated using the 3-(4,5-dimethylthiazol-2-yl)-2,5-diphenyltetrazolium bromide (MTT) method.[48] CXCR4-antagonistic activity was evaluated by the inhibition of [^{125}I]-SDF-1-binding to CXCR4 transfectants of CHO cells.[49] **37a**, an (L-Arg-L-Nal)-type EADI containing FC131 analogue, showed moderate anti-HIV activity (EC_{50} = 2.4 μM) and CXCR4-antagonistic activity (100 μM > IC_{50} > 31 μM). Introduction of an EADI into the Arg-Nal sequence caused a remarkable decrease in anti-HIV activity (33-fold lower activity). NMR and simulated annealing molecular dynamics (SA-MD) analysis of **37a** showed a pseudopeptide backbone structure with a nearly symmetrical pentagonal shape similar to that of FC131,[16] excluding the difference between the orientation of two protons in the (*E*)-alkene unit of **37a** and that of the carbonyl oxygen/amino proton in the Arg-Nal amide bond of FC131 (Figure 2a).[50] Substitution for the amide bond with the EADI caused an inversion of the olefinic plane (180° rotation of pseudo ψ and ϕ bonds), possibly due to dissolution of the 1,3-pseudo-allylic strain between the carbonyl group of Arg and the side chain of Nal. Introduction of an EADI into the Arg-D-Nal sequence of **37e** (an FC131 epimer, EC_{50} = 1.9 μM, IC_{50} = 190 nM) also caused a significant but moderate decrease in anti-HIV activity (the activity of **37f** is 5-fold lower than that of **37e**). The amide bonds of the Arg-L/D-Nal sequences were necessary for high potency. These results suggested that either a deletion of the hydrogen bond interaction with CXCR4 by the insertion of an EADI or an increase in hydrophobicity might be unsuitable. **37b**, an (L-Arg-L-Nal)-type RADI-containing FC131 analogue, did not show anti-HIV or CXCR4-antagonistic activity up to the concentration of 100 μM, suggesting that the planar nature of the amide bond is critical to maintain the pentagonal global conformation for high anti-HIV activity and that the replacement of the amide bond with RADI causes a conformational change of FC131. **37c**, an (L-Nal-Gly)-type EADI-containing FC131 analogue, showed almost the same anti-HIV activity (EC_{50} = 2.4 μM) as **37a** containing an (L-Arg-L-Nal)-type EADI. NMR and SA-MD analysis of **37c** showed a similar backbone structure with FC131 (Figure 2b).[50] The Nal-Gly amide bond was replaced by the EADI without an inversion of the olefinic plane. **37d**, an (L-Nal-Gly)-type RADI-containing FC131 analogue, exhibited relatively higher anti-HIV and CXCR4-antagonistic activities (EC_{50} = 0.98 μM, IC_{50} = 32 nM) than **37c** (IC_{50} = 180 nM), although these activities were weaker than those of FC131. These results also indicated an importance of the amide bond of the Nal-Gly sequence, as in the case of the Arg-Nal amide bond.

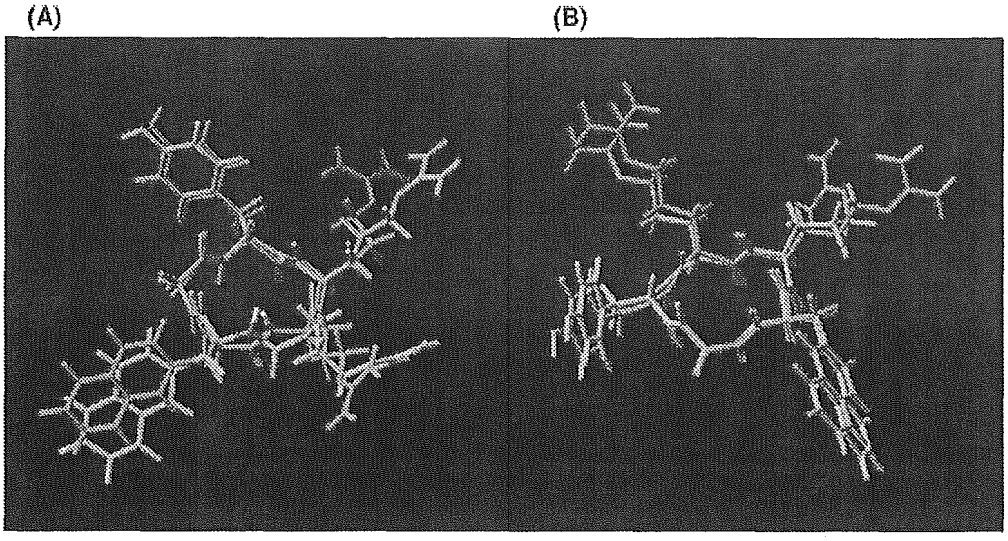

Figure 2. Superimpositions of low-energy structures of FC131 and **37a** (A) or **37c** (B). The FC131 structure is depicted in green, and the **37a** or **37c** structure is depicted in purple.

Conclusion

A set of (L-Arg-L/D-Nal)-type EADIs were synthesized from a single substrate of γ,δ-*cis*-γ,δ-epimino (*E*)-α,β-enoate by combination of MSA-mediated aziridinyl ring-opening reactions and *anti*-S_N2' reactions with organozinc−copper reagents that were prepared from 2-naphthylmethylZnBr and CuCN. Organozinc−copper-mediated α-alkylation reactions are thought to be useful for construction of several side chains at the α-position of EADIs, as organocopper-mediated α-alkylation reactions that have been generally used. Next, EADIs and RADIs of Arg-Nal and Nal-Gly, including the above EADIs, were synthesized and inserted into cyclic pentapeptides, FC131 analogues, to disclose biological importance of each amide bond. The present results will be useful for the development of nonpeptide CXCR4 antagonists derived from FC131. It is also noteworthy that EADI units were introduced into cyclic pentapeptides without any significant conformational changes in the pentagonal backbone structures, except for those of substituted (*E*)-alkene units, suggesting that the planar nature of (*E*)-alkene units caused the conformational maintenance of the backbones excluding the olefinic moiety. SA-MD analysis showed that the parent peptide (FC131) and the EADI-introduced pseudopeptides (**37a** and **37c**) have nearly equal distances between any two β-carbons in all of the side chains. It suggests that these compounds maintain similar dispositions of pharmacophores and that the biological differences between these compounds are derived from the (*E*)-alkene/amide bond units. As such, EADIs become useful tools for investigation of biological contributions of amide bonds.

Experimental Section

General. Melting points are uncorrected. ^{1}H NMR spectra were recorded using a JEOL EX-270, a JEOL AL-400, or a Bruker AM 600 spectrometer at 270, 400, or 600 MHz ^{1}H frequency in $CDCl_3$, respectively. Chemical shifts are reported in parts per million downfield from internal tetramethylsilane. Nominal (LRMS) and exact mass (HRMS) spectra were recorded on a JEOL JMS-01SG-2 or JMS-HX/HX 110A mass spectrometer. Ion-spray (IS)-mass spectrum was obtained with a Sciex API *III*E triple quadrupole mass spectrometer (Toronto, Canada). Optical rotations were measured in $CHCl_3$ or H_2O with a JASCO DIP-360 digital polarimeter (Tokyo, Japan) or a Horiba high-sensitive polarimeter SEPA-200 (Kyoto, Japan). For flash column chromatography, silica gel 60 H (silica gel for thin-layer chromatography, Merck) and Wakogel C-200 (silica gel for column chromatography) were employed. HPLC solvents were H_2O and MeCN, both containing 0.1% (v/v) TFA. For analytical HPLC, a Cosmosil 5C18-AR column (4.6 mm × 250 mm, Nacalai Tesque Inc., Kyoto, Japan) was eluted with a linear gradient of MeCN at a flow rate of 1 mL/min on a Waters model 600 (Nihon Millipore, Ltd., Tokyo, Japan). Preparative HPLC was performed on a Waters Delta Prep 4000 equipped with a Cosmosil 5C18-AR column (20 mm × 250 mm, Nacalai Tesque Inc.) using an isocratic mode of MeCN at a flow rate of 15 mL/min.

Boc-Arg(Mts)-OMe, 5. To a stirred solution of Boc-Arg(Mts)-OH (10.0 g, 21.9 mmol) in DMF (50 mL) at 4 °C were added potassium bicarbonate (4.39 g, 43.8 mmol) and methyl iodide (2.73 mL, 43.8 mmol), and the mixture was stirred at room temperature for 10 h. The reaction mixture was concentrated under reduced pressure. The residue was extracted with EtOAc, and the extract was washed successively with saturated citric acid, brine, saturated aqueous $NaHCO_3$, and brine and dried over $MgSO_4$. Concentration under reduced pressure gave 10.4 g (21.8 mmol, 100%) of methyl ester **5** as a yellow oil.

$[\alpha]^{22}_D$ −4.25 (*c* 0.47, $CHCl_3$). ^{1}H NMR (270 MHz, $CDCl_3$) δ: 1.42 (9H, s, *tert*-Bu), 1.61 (2H, br m, CH_2), 1.78 (2H, br m, CH_2), 2.59 (3H, s, Ar-*p*-Me), 2.66 (6H, s, Ar-*o*-Me), 3.22 (2H, br m, CH_2), 3.73 (3H, s, OMe), 4.21−4.28 (1H, m, CH), 5.23 (1H, d, J = 8.2 Hz, NH), 6.14 (3H, br, guanidino), 6.89 (2H, s, ArH). *m/z* (FAB-LRMS): 471 (MH^+), 415, 371, 289 (base peak), 119. Found (FAB-HRMS): 471.2268. Calcd for $C_{21}H_{35}O_6N_4S$ (MH^+): 471.2277.

***N*-*tert*-Butoxy-[2(*S*)-hydroxy-1(*S*)-[3-[[imino[[(2,4,6-trimethylphenyl)sulfonyl]amino]methyl]amino]propyl]but-3-enyl]formamide, 6.** To a stirred solution of Boc-Arg(Mts)-OMe, **5** (5.0 g, 10.6 mmol), in toluene/CH_2Cl_2 (1:1 (v/v) 100 mL) was added dropwise a solution of DIBAL-H in toluene (1.0 M, 32 mL, 32 mmol) at −50 °C under argon, and the mixture was stirred at −78 °C for 2 h. To the solution, was added dropwise a vinyl Grignard (CH_2=CHMgCl) reagent in THF (13 mL, 32 mmol) at −78 °C, and the mixture was stirred for 6 h with a gradual warming to 0 °C. The reaction was quenched with saturated aqueous citric acid at −78 °C, and organic solvents were concentrated under reduced pressure. The residue was extracted with EtOAc, and the extract was washed successively with saturated aqueous citric acid, satu-

rated aqueous $NaHCO_3$, and brine and dried over $MgSO_4$. Concentration under reduced pressure followed by flash column chromatography over silica gel with EtOAc/*n*-hexane (2:1) gave a *threo*-allyl alcohol **6** and an *erythro*-allyl alcohol (2*R* isomer of **6**) (12:1), in order of elution (**6**, 1.5 g, 30% yield from **5**).

Compound **6**: colorless oil. $[\alpha]^{22}_D$ −15.74 (*c* 0.63, $CHCl_3$). ^1H NMR (270 MHz, $CDCl_3$) δ: 1.40 (9H, s, *tert*-Bu), 1.57 (2H, br m, 2-CH_2), 1.70 (2H, br m, 1-CH_2), 2.26 (3H, s, Ar-*p*-Me), 2.66 (6H, s, Ar-*o*-Me), 3.24 (2H, br m, 3-CH_2), 3.55 (1H, br, 1-H), 4.08 (1H, br, 2-H), 4.97 (1H, d, J = 9.7 Hz, NH), 5.18 (1H, d, J = 10.5 Hz, C*H*H=), 5.28 (1H, d, J = 17.3 Hz, CH*H*=), 5.77−5.89 (1H, m, CH=), 6.20 (3H, br, guanidino), 6.89 (2H, s, ArH). *m/z* (ISMS): 469.5 (MH^+). Found (FAB-HRMS): 469.2490. Calcd for $C_{22}H_{37}O_5N_4S$ (MH^+): 469.2485.

Compound 2*R* isomer of **6**: colorless oil. $[\alpha]^{21}_D$ −4.57 (*c* 2.84, $CHCl_3$). ^1H NMR (270 MHz, $CDCl_3$) δ: 1.41 (9H, s, *tert*-Bu), 1.48 (2H, br m, 2-CH_2), 1.64 (2H, br m, 1-CH_2), 2.30 (3H, s, Ar-*p*-Me), 2.63 (6H, s, Ar-*o*-Me), 3.15 (2H, br m, 3-CH_2), 3.63 (1H, br, 1-H), 4.18 (1H, br, 2-H), 5.12 (1H, br, NH), 5.24 (1H, d, J = 10.5 Hz, CH*H*=), 5.32 (1H, d, J = 17.0 Hz, C*H*H=), 5.74−5.85 (1H, m, CH=), 6.32 (3H, br, guanidino), 6.95 (2H, s, ArH). *m/z* (ISMS): 469.5 (MH^+).

[2(*S*)-Hydroxy-1(*S*)-[3-[[imino[[(2,4,6-trimethylphenyl)-sulfonyl]amino]methyl]amino]propyl]but-3-enyl][(2-nitrophenyl)sulfonyl]amine, 7. To a mixture of allyl alcohol **6** (4.2 g, 9.0 mmol) and anisole (0.97 mL, 9.0 mmol) at 0 °C was added 4 M HCl/dioxane (100 mL), and the mixture was stirred at room temperature for 2 h. The mixture was concentrated under reduced pressure. To a stirred solution of the residue in $CHCl_3$ (20 mL) at 0 °C were added 2-nitrobenzenesulfonyl chloride (2.38 g, 10.8 mmol), triethylamine (Et_3N) (5 mL), and pyridine (20 mL), and the mixture was allowed to warm to room temperature, stirred at this temperature for 12 h, and extracted with $CHCl_3$. The extract was washed with saturated aqueous citric acid, saturated aqueous $NaHCO_3$, and brine and dried over $MgSO_4$. Concentration under reduced pressure followed by chromatography over silica gel with $CHCl_3$/MeOH (18:1) gave 3.2 g (5.8 mmol, 65% from **6**) of **7** as a yellow oil.

$[\alpha]^{28}_D$ −57.79 (*c* 1.83, $CHCl_3$). ^1H NMR (270 MHz, $CDCl_3$) δ: 1.61 (4H, br m, 1, 2-CH_2), 2.27 (3H, s, Ar-*p*-Me), 2.64 (6H, s, Ar-*o*-Me), 3.15 (2H, br m, 3-CH_2), 3.50 (1H, br, 1-H), 3.72−3.78 (1H, m, 2-H), 4.72 (1H, d, J = 10.5 Hz, C*H*H=), 5.07 (1H, d, J = 17.0 Hz, CH*H*=), 5.42−5.48 (1H, m, CH=), 5.90 (1H, d, J = 8.1 Hz, NH), 6.26 (3H, br, guanidino), 6.90 (2H, s, ArH), 7.65−7.69 (2H, m, ArH), 7.78−7.82 (1H, m, ArH), 8.04−8.08 (1H, m, ArH). *m/z* (ISMS): 554.5 (MH^+). Found (FAB-HRMS): 554.1735. Calcd for $C_{23}H_{32}O_7N_5S_2$ (MH^+): 554.1743.

3(*S*)-[3-[[Imino[[(2,4,6-trimethylphenyl)sulfonyl]amino]methyl]amino]propyl]-1-[(2-nitrophenyl)sulfonyl]-2(*R*)-vinylaziridine, 8. To a stirred solution of allyl alcohol **7** (3.1 g, 5.6 mmol) in dry THF (30 mL) at 0 °C were added triphenylphosphine (1.6 g, 6.2 mmol) and diethyl azodicarbonate (2.4 mL of a 40% solution in toluene, 6.2 mmol), and the reaction mixture was stirred at this temperature for 30 min. The mixture was concentrated under reduced pressure and purified by chromatography over silica gel with EtOAc/*n*-hexane (2:1) to give 2.8 g (5.2 mmol, 93% yield from **7**) of aziridine **8** as a yellow oil.

$[\alpha]^{23}_D$ −10.45 (*c* 2.20, $CHCl_3$). ^1H NMR (270 MHz, $CDCl_3$) δ: 1.48 (4H, br m, 1, 2-CH_2), 2.26 (3H, s, Ar-*p*-Me), 2.65 (6H, s, Ar-*o*-Me), 3.02 (1H, br, 2-H), 3.15 (2H, br m, 3-CH_2), 3.46 (1H, br, 3-H), 5.29 (1H, d, J = 9.7 Hz, C*H*H=), 5.42 (1H, d, J = 17.0 Hz, CH*H*=), 5.45−5.53 (1H, m, CH=), 6.41 (3H, br, guanidino), 6.88 (2H, s, ArH), 7.45−7.50 (2H, m, ArH), 7.54−7.75 (2H, m, ArH). *m/z* (ISMS): 536.5 (MH^+). Found (FAB-HRMS): 536.1630. Calcd for $C_{23}H_{30}O_6N_5S_2$ (MH^+): 536.1638.

Phenylmethyl 3-3(*S*)-[3-[[Imino[[(2, 4, 6-trimethylphenyl)sulfonyl]amino]methyl]amino]propyl]-2(*R*)-[(2-nitrophenyl)sulfonyl-2-aziridinyl]prop-2-enoate, 9. To a solution of aziridine **8** (1.2 g, 2.2 mmol) in CH_2Cl_2 (30 mL) was bubbled O_3 gas at −78 °C until a blue color persisted. To the above solution was added Me_2S (1.7 mL, 22 mmol), and the mixture was stirred for 30 min and then dried over $MgSO_4$. Concentration under reduced pressure gave an oily residue of a crude aldehyde, which was used immediately in the next step without further purification. To a stirred suspension of LiCl (230 mg, 5.4 mmol) in MeCN (5 mL) under argon, were added $(EtO)_2P(O)CH_2CO_2Bn$ (1.5 mL, 5.4 mmol) and $(^iPr)_2NEt$ (DIPEA) (0.94 mL, 5.4 mmol) at 0 °C. After 20 min, the above aldehyde in MeCN (15 mL) was added to the mixture at 0 °C, and the mixture was stirred at this temperature for 8 h. The mixture was concentrated under reduced pressure, and the residue was extracted with EtOAc. The extract was washed successively with saturated aqueous citric acid and H_2O and dried over $MgSO_4$. Concentration under reduced pressure followed by chromatography over silica gel with $CHCl_3$/MeOH (40:1) gave the title compound **9** (1.0 g, 1.5 mmol, 67% yield from **8**) as a colorless oil.

$[\alpha]^{23}_D$ −10.1 (*c* 1.49, $CHCl_3$). ^1H NMR (270 MHz, $CDCl_3$) δ: 1.63 (4H, br m, 1, 2-CH_2), 2.17 (3H, s, Ar-*p*-Me), 2.64 (6H, s, Ar-*o*-Me), 3.20 (2H, br m, 3-CH_2), 3.22 (1H, br, 2-H), 3.61 (1H, br, 3-H), 5.15 (2H, s, CH_2), 6.18 (1H, dd, J = 15.7, 0.8 Hz, CH=), 6.22 (3H, br, guanidino), 6.66 (1H, dd, J = 15.5, 6.9 Hz, CH=), 6.88 (2H, s, ArH), 7.34 (5H, s, ArH), 7.56−7.60 (1H, m, ArH), 7.71−7.79 (2H, m, ArH), 8.13−8.17 (1H, m, ArH). *m/z* (ISMS): 670.5 (MH^+). Found (FAB-HRMS): 670.2019. Calcd for $C_{31}H_{36}O_8N_5S_2$ (MH^+): 670.2005.

Phenylmethyl 8-[[Imino[[(2,4,6-trimethylphenyl)sulfonyl]amino]methyl]amino]-5(*S*)-[[(2-nitrophenyl)sulfonyl]amino]-2(*R*)-(naphthylmethyl)oct-3-enoate [Ns-L-Arg(Mts)-ψ[(*E*)-CH=CH]-L-Nal-OBn], 10. To a stirred solution of CuCN (219 mg, 2.45 mmol) and LiCl (207 mg, 4.89 mmol) in dry THF (3.0 mL) under argon at −78 °C, was added dropwise 0.5 M (2-naphthylmethyl)zincbromide in THF solution (4.9 mL, 2.45 mmol), and the mixture was stirred at 0 °C for 10 min. A solution of enoate **9** (273 mg, 0.408 mmol) in dry THF (9.0 mL) was added dropwise to the above mixture at −78 °C with stirring, and the stirring was continued for 30 min followed by quenching with 10 mL of a 1:1 saturated aqueous NH_4Cl/28% NH_4OH solution. The mixture was extracted with Et_2O, and the extract was washed with saturated aqueous NH_4Cl and brine and dried over $MgSO_4$. Concentration under reduced pressure gave an oily residue, which was purified by chromatography over silica gel with *n*-hexane/EtOAc (1:2) to yield 273 mg (0.337 mmol, 83% yield from **9**) of compound **10** as a yellow oil. $[\alpha]^{33}_D$ −80.9 (*c* 0.61, $CHCl_3$). ^1H NMR (270 MHz, $CDCl_3$) δ: 1.35 (2H, br m, 2-CH_2), 1.55 (2H, br m, 1-CH_2), 2.04 (3H, s, Ar-*p*-Me), 2.26 (6H, s, Ar-*o*-Me), 2.97 (2H, br, CH_2), 2.98 (2H, br m, 3-CH_2), 3.20−3.25 (1H, m, 2-H), 3.90 (1H, br, 5-H), 4.93 (2H, s, CH_2), 5.24 (1H, dd, J = 15.5, 6.9 Hz, CH=), 5.50 (1H, dd, J = 15.4, 8.4 Hz, CH=), 5.67 (1H, d, J = 4.6 Hz, NH), 5.95 (3H, br, guanidino), 6.89 (2H, s, ArH), 7.05−7.28 (7H, m, ArH), 7.42−7.77 (9H, m, ArH), 7.96−8.00 (1H, m, ArH). *m/z* (ISMS): 814.0 (MH^+). Found (FAB-HRMS): 812.2803. Calcd for $C_{42}H_{46}O_8N_5S_2$ (MH^+): 812.2788.

Phenylmethyl 5(*S*)-[(Fluoren-9-ylmethoxy)carbonyl-amino]-8-[[imino[[(2,4,6-trimethylphenyl)sulfonyl]amino]methyl]amino]-2(*R*)-(2-naphthylmethyl)oct-3-enoate [Fmoc-L-Arg(Mts)-ψ[(*E*)-CH=CH]-L-Nal-OBn], 11. To a stirred solution of enoate **10** (81 mg, 0.10 mmol) in DMSO/MeCN (1:49, 5 mL), were added thiophenol (31 μL, 0.3 mmol) and K_2CO_3 (55 mg, 0.4 mmol) at room temperature, and the mixture was stirred at 50 °C for 1 h. The solution was filtered, and the filtrate was concentrated under reduced pressure. The residue was extracted with EtOAc, washed with brine, and dried over $MgSO_4$. Concentration under reduced pressure gave an oily residue, which was dissolved in THF/H_2O (1:1, 50 mL). Fmoc-OSu (33 mg, 0.1 mmol) and Et_3N (27 μL, 0.19 mmol) were added to the above solution at 0 °C. After being stirred for 6 h, the mixture was acidified with 0.1 M HCl and then extracted with EtOAc. The extract was washed with 0.1 M HCl and brine and dried over $MgSO_4$. Concentration under reduced pressure followed by chromatography over silica gel with *n*-hexane/EtOAc (1:2) gave the title compound **11** (60 mg, 70.9 μmol, 71% yield from **10**) as a colorless oil.

$[\alpha]^{29}_D$ −11.2 (*c* 0.63, $CHCl_3$). ^1H NMR (270 MHz, $CDCl_3$) δ: 1.26 (4H, br m, 1, 2-CH_2), 2.18 (3H, s, Ar-*p*-Me), 2.63 (6H, s,

Ar-*o*-Me), 2.94 (2H, br, CH_2), 3.19 (2H, br m, 3-CH_2), 3.38 (1H, br, 2-H), 3.96 (1H, br, 5-H), 4.12 (1H, t, J = 5.8 Hz, ArH), 4.35 (2H, t, J = 5.94 Hz, CH_2), 4.82 (1H, br, NH), 5.01 (2H, s, CH_2), 5.24 (1H, dd, J = 15.0, 5.7 Hz, CH=), 5.64 (1H, dd, J = 14.4, 7.8 Hz, CH=), 6.16 (3H, br, guanidino), 6.81 (2H, s, ArH), 7.08–7.28 (8H, m, ArH), 7.33–7.42 (4H, m, ArH), 7.42–7.54 (3H, m, ArH), 7.64–7.74 (5H, m, ArH). *m/z* (ISMS): 850.0 (MH^+). Found (FAB-HRMS): 849.3664. Calcd for $C_{51}H_{53}O_6N_4S_2$ (MH^+): 849.3686.

5(*S*)-[(Fluoren-9-ylmethoxy)carbonylamino]-8-[[imino-[[(2, 4, 6-trimethylphenyl)sulfonyl]amino]methyl]amino]-2(*R*)-(2-naphthylmethyl)oct-3-enoic Acid [Fmoc-L-Arg-(Mts)-ψ[(*E*)-CH=CH]-L-Nal-OH], 12. The enoate **11** (30 mg, 0.037 mmol) was dissolved in TFA (10 mL), and thioanisole (500 μL), *m*-cresol (200 μL), and 1,2-ethanedithiol (100 μL) were added to the solution at 0 °C, and the mixture was stirred for 12 h at room temperature. The mixture was concentrated under reduced pressure and extracted with EtOAc. The extract was washed with brine and dried over $MgSO_4$. Concentration under reduced pressure followed by chromatography over silica gel with *n*-hexane/EtOAc (1:4) gave the title compound **12** (28 mg, 0.036 mmol, 98% yield from **11**) as a colorless oil.

$[\alpha]^{23}_D$ −15.2 (*c* 0.07, $CHCl_3$). ^1H NMR (600 MHz, $CDCl_3$) δ: 1.25 (4H, br m, 1, 2-CH_2), 2.20 (3H, s, Ar-*p*-Me), 2.62 (6H, s, Ar-*o*-Me), 2.86 (2H, br, CH_2), 3.05 (2H, br m, 3-CH_2), 3.49 (1H, br, 2-H), 3.68 (1H, br, 5-H), 4.10 (1H, br, ArH), 4.20–4.26 (2H, m, CH_2), 4.93 (1H, br, CH=), 5.34 (1H, br, CH=), 5.38 (1H, br, NH), 5.95 (3H, br, guanidino), 6.84 (2H, s, ArH), 7.20–7.41 (7H, m, ArH), 7.48–7.57 (3H, m, ArH), 7.65–7.77 (5H, m, ArH). *m/z* (ISMS): 760.0 (MH^+). Found (FAB-HRMS): 759.3228. Calcd for $C_{44}H_{47}O_6N_4S_2$ (MH^+): 759.3216.

Phenylmethyl 8-[[Imino[[(2, 4, 6-trimethylphenyl)sulfonyl]amino]methyl]amino]-5(*S*)-[[(2-nitrophenyl)-sulfonyl]amino]-2(*S*)-(naphthylmethyl)oct-3-enoate [Ns-L-Arg(Mts)-ψ[(*E*)-CH=CH]-D-Nal-OBn], 14. To a stirred solution of enoate **9** (500 mg, 0.75 mmol) in $CHCl_3$ (5 mL) was added dropwise MSA (435 μL, 6.7 mmol) at room temperature with stirring, and the stirring was continued for 20 min. The mixture was extracted with EtOAc, and the extract was washed successively with aqueous 5% citric acid, water, aqueous 5% $NaHCO_3$, and water and dried over $MgSO_4$. Concentration under reduced pressure gave an oily residue of the crude mesylate **13**, which was used directly in the following step without further purification. To a stirred slurry of CuCN (269 mg, 3.0 mmol) in dry THF (5 mL) under argon at −78 °C was added dropwise (2-naphthylmethyl)zincbromide in THF solution (6.0 mL, 3.0 mmol), and the mixture was stirred at 0 °C for 15 min followed by addition of $BF_3{\cdot}Et_2O$ (369 μL, 3.0 mmol) at −78 °C and then stirred at −78 °C for 15 min. To the mixture at −78 °C with stirring was added by syringe a solution of the crude mesylate **13** in THF (10 mL), and the stirring was continued at −78 °C for 1 h followed by quenching with saturated aqueous NH_4Cl and aqueous 28% NH_4OH (1:1) at 0 °C. The mixture was allowed to warm to room temperature and extracted with Et_2O. The extract was washed with H_2O, dried over $MgSO_4$, and concentrated under reduced pressure. The residue was purified by chromatography over silica gel with *n*-hexane/EtOAc (1:2) to give 408 mg (0.50 mmol, 67% from **9**) of protected EADI **14** as a yellow oil. $[\alpha]^{32}_D$ −41.7 (*c* 0.60, $CHCl_3$). ^1H NMR (270 MHz, $CDCl_3$) δ: 1.54 (4H, br m, 1, 2-CH_2), 2.25 (3H, s, Ar-*p*-Me), 2.66 (6H, s, Ar-*o*-Me), 2.86 (2H, br m, 3-CH_2), 2.98–3.06 (2H, m, CH_2), 3.15–3.23 (1H, m, 2-H), 3.78–3.88 (1H, m, 5-H), 4.98 (2H, s, CH_2), 5.09 (1H, dd, J = 15.5, 8.0 Hz, CH=), 5.49 (1H, dd, J = 15.5, 8.2 Hz, CH=), 5.57 (1H, d, J = 8.4 Hz, NH), 6.09 (3H, br, guanidino), 6.89 (2H, s, ArH), 7.10–7.26 (7H, m, ArH), 7.37–7.76 (9H, m, ArH), 7.95–7.98 (1H, m, ArH). *m/z* (ISMS): 814.0 (MH^+). Found (FAB-HRMS): 812.2775. Calcd for $C_{42}H_{46}O_8N_5S_2$ (MH^+): 812.2788.

Phenylmethyl 5(*S*)-[(Fluoren-9-ylmethoxy)carbonyl-amino]-8-[[imino[[(2,4,6-trimethylphenyl)sulfonyl]amino]methyl]amino]-2(*S*)-(2-naphthylmethyl)oct-3-enoate [Fmoc-L-Arg(Mts)-ψ[(*E*)-CH=CH]-D-Nal-OBn], 15. By use of a procedure identical with that described for the preparation of **12** from **10**, the enoate **14** (30 mg, 37 μmol) was converted into 28 mg (36 μmol, 98% yield from **14**) of the title compound **15** as a colorless oil.

$[\alpha]^{29}_D$ −1.6 (*c* 0.61, $CHCl_3$). ^1H NMR (270 MHz, $CDCl_3$) δ: 1.14–1.30 (4H, br m, 1, 2-CH_2), 2.17 (3H, s, Ar-*p*-Me), 2.62 (6H, s, Ar-*o*-Me), 2.91 (2H, br m, 3-CH_2), 3.15–3.23 (2H, m, CH_2), 3.40 (1H, br, 2-H), 3.95 (1H, br, 5-H), 4.11 (1H, t, J = 6.5 Hz, ArH), 4.33 (2H, d, J = 5.7 Hz, CH_2), 4.85 (1H, d, J = 6.8 Hz, NH), 5.00 (2H, s, CH_2), 5.25 (1H, dd, J = 16.7, 6.8 Hz, CH=), 5.61 (1H, dd, J = 14.3, 7.6 Hz, CH=), 6.13 (3H, br, guanidino), 6.81 (2H, s, ArH), 7.09–7.27 (8H, m, ArH), 7.32–7.45 (4H, m, ArH), 7.46–7.56 (3H, m, ArH), 7.64–7.73 (5H, m, ArH). *m/z* (ISMS): 850.0 (MH^+). Found (FAB-HRMS): 849.3698. Calcd for $C_{51}H_{53}O_6N_4S_2$ (MH^+): 849.3686.

5(*S*)-[(Fluoren-9-ylmethoxy)carbonylamino]-8-[[imino-[[(2, 4, 6-trimethylphenyl)sulfonyl]amino]methyl]amino]-2(*S*)-(2-naphthylmethyl)oct-3-enoic Acid [Fmoc-L-Arg-(Mts)-ψ[(*E*)-CH=CH]-D-Nal-OH], 16. By use of a procedure identical with that described for the preparation of **12** from **11**, the enoate **15** (153 mg, 0.19 mmol) was converted into 144 mg (0.19 mmol, 99% yield from **15**) of the title compound **16** as a colorless oil.

$[\alpha]^{23}_D$ 10.8 (*c* 0.19, $CHCl_3$). ^1H NMR (270 MHz, $CDCl_3$) δ: 1.24 (4H, br m, 1, 2-CH_2), 2.17 (3H, s, Ar-*p*-Me), 2.70 (6H, s, Ar-*o*-Me), 2.90 (2H, br m, 3-CH_2), 3.07 (2H, m, CH_2), 3.29 (1H, br, 2-H), 3.67 (1H, br, 5-H), 4.06 (1H, t, J = 8.2 Hz, ArH), 4.28 (2H, d, J = 5.9 Hz, CH_2), 5.12 (1H, d, J = 5.9 Hz, NH), 5.26 (1H, dd, J = 15.0, 5.8 Hz, CH=), 5.59 (1H, dd, J = 15.0, 8.0 Hz, CH=), 6.19 (3H, br, guanidino), 6.80 (2H, s, ArH), 7.18–7.40 (7H, m, ArH), 7.46–7.54 (3H, m, ArH), 7.59–7.70 (5H, m, ArH). *m/z* (ISMS): 760.0 (MH^+). Found (FAB-HRMS): 759.3201. Calcd for $C_{44}H_{47}O_6N_4S_2$ (MH^+): 759.3216.

H-D-Tyr(O^{t}Bu)-Arg(Pbf)-Arg(Mts)-ψ[(*E*)-CH=CH]-Nal-Gly-NHNHCO−Wang Resin. *p*-Nitrophenyl carbonate Wang resin **33** (Calbiochem-Novabiochem Japan, Ltd., Tokyo, Japan, 0.93 mmol/g, 323 mg, 0.3 mmol) was treated with $NH_2NH_2{\cdot}H_2O$ (146 μL, 3.0 mmol) in DMF (3 mL) at room temperature for 2 h to give a hydrazide linker **34**. Protected peptide−resins were manually constructed by Fmoc-based solid-phase peptide synthesis. ^{t}Bu for Tyr and Mts or Pbf for Arg were employed for side-chain protection. Fmoc deprotection was achieved by 20% piperidine in DMF (1 min × 2 and 15 min × 1). Fmoc−amino acids including EADIs or RADIs were condensed to free amino groups by treatment with 3 equiv of reagents (Fmoc−amino acid, *N,N'*-diisopropylcarbodiimide (DIPCDI) and HOBt·H_2O) in DMF for 1.5 h.

***cyclo*(-D-Tyr-Arg-Arg-ψ[(*E*)-CH=CH]-Nal-Gly-)·2TFA (37a).** The protected **37a** resin (34 mg, 0.025 mmol) was treated with TFA (0.5 mL) in $CHCl_3$ (4.5 mL) at room temperature for 2 h, and the mixture was filtered. Concentration of the filtrate under reduced pressure gave a crude hydrazide (H-D-Tyr-Arg(Pbf)-Arg(Mts)-ψ[(*E*)-CH=CH]-Nal-Gly-$NHNH_2$) as a colorless powder. To a stirred solution of the hydrazide in DMF (1 mL) were added a solution of 4 M HCl in DMF (16.6 μL, 75 μmol) and isoamyl nitrite (40 μL, 0.20 mmol) at −30 °C. After being stirred at −10 °C for 20 min, the mixture was diluted with precooled DMF (50 mL). To the above solution was added DIPEA (191 μL, 1.1 mmol) at −30 °C, and the mixture was stirred for 48 h at −20 °C. Concentration under reduced pressure gave a yellow oil (crude *cyclo*(-D-Tyr-Arg(Pbf)-Arg(Mts)-ψ[(*E*)-CH=CH]-Nal-Gly-)). To the protected cyclic peptide were added *m*-cresol (0.4 mL, 3.6 mmol), 1, 2-ethanedithiol (160 μL, 1.9 mmol), thioanisole (1.0 mL, 8.5 mmol), TFA (10 mL), and bromotrimethylsilane (1.2 mL, 9.1 mmol) at 0 °C, and the stirring was continued at room temperature for 12 h. Concentration under reduced pressure and purification by preparative HPLC gave the cyclic pseudopeptide **37a** (8.5 mg, 36% yield from protected **37a** resin) as a freeze-dried powder.

$[\alpha]^{27}_D$ −53.3 (*c* 0.24, H_2O). t_R = 28.6 min (linear gradient of MeCN in H_2O, 10 to 40% over 30 min). *m/z* (ISMS): 714.0 (MH^+). Found (FAB-HRMS): 713.3879. Calcd for $C_{37}H_{49}O_5N_{10}$ (MH^+): 713.3887.

***cyclo*(-D-Tyr-Arg-Arg-ψ[(*E*)-CH=CH]-D-Nal-Gly-)·2TFA (37f).** By use of a procedure identical with that described